Overexpression of Long Non-Coding RNA AP001505.9 Inhibits Dedifferentiation in Human Hyaline Chondrocyte

Lin Chen
Jilin University https://orcid.org/0000-0002-2011-2048
Jinying Xu
Jilin University
Shuang Lv
Jilin University
Yan Zhao
Jilin University
Dongjie Sun
Jilin University
Yangyang Zheng
Jilin University
Xianglan Li
Jilin University
Lihong Zhang
Jilin University
Guangfan Chi
Jilin University
Yulin Li (ylli@jlu.edu.cn)
China-Japan Union Hospital of Jilin University

Research article

Keywords: Long noncoding RNA, dedifferentiation, chondrocyte, autologous 44 chondrocyte implantation, osteoarthritis, microRNA

Posted Date: August 24th, 2020

DOI: https://doi.org/10.21203/rs.3.rs-61734/v1

Overexpression of long non-coding RNA AP001505.9 inhibits dedifferentiation in human hyaline chondrocyte

Lin Chen[1, 2], Jinying Xu[1], Shuang Lv[1], Yan Zhao[1,3], Dongjie Sun[1], Yangyang Zheng[1], Xianglan Li[1,4], Lihong Zhang[1], Guangfan Chi[1]*, Yulin Li[1]*

[1]The Key Laboratory of Pathobiology, Ministry of Education, College of Basic Medical Sciences, Jilin University, 126 Xinmin Street, Changchun, Jilin, China

[2]Department of Gastrointestinal and Colorectal Surgery, China-Japan Union Hospital of Jilin University, 126 Xiantai Street, Changchun, Jilin, China

[3]Department of Operating Room, China-Japan Union Hospital of Jilin University, 126 Xiantai Street, Changchun, Jilin, China

[4]Department of Dermatology, China-Japan Union Hospital of Jilin University, 126 Xiantai Street, Changchun, Jilin, China

*Address correspondence to Yulin Li, +8613904312889, fax number: 0431-85619469, email: ylli@jlu.edu.cn; or Guangfan Chi, +8613756482684, email: guangfan130@jlu.edu.cn, ORCID: https://orcid.org/0000-0001-7096-9106.

Abstract

Background: Autologous chondrocyte implantation (ACI) requires a large number of human hyaline chondrocytes. Unfortunately, human hyaline chondrocytes often undergo dedifferentiation in vitro. Long non-coding RNAs (lncRNA) play a

regulatory role in gene expression in many pathological and physiological processes. However, their role in human hyaline chondrocyte dedifferentiation remains unclear. This study aimed to investigate the expression profiles of lncRNAs in human hyaline chondrocyte dedifferentiation.

Methods: Human hyaline chondrocytes were cultured in vitro and screened for the occurrence of dedifferentiation using real-time quantitative PCR (qPCR), immunofluorescence, and western blotting. The expression profiles of lncRNAs and mRNAs during dedifferentiation were analyzed by microarray analysis and real-time qPCR. We used pellet culture to redifferentiate chondrocytes and the expression of related lncRNAs were assessed. The function of lncRNA AP001505.9 (ENST00000569966) was determined by overexpression, fluorescence in situ hybridization, competing endogenous RNA (ceRNA) analysis, and double luciferase labeling.

Results: We probed human hyaline chondrocytes dedifferentiation and identified 334 upregulated and 381 downregulated lncRNAs. The expression of downregulated lncRNA AP001505.9 in dedifferentiation was reversed by pellet culture. The overexpression of AP001505.9 inhibited dedifferentiation by promoting the expression of SRY-Box transcription factor 9 (SOX-9) and inhibiting the expression of type I collagen (COL1) both in vitro and in vivo.

Conclusion: This study reveals for the first time the expression profiles of lncRNAs in human hyaline chondrocyte dedifferentiation, thereby providing a new perspective

for exploring the potential mechanism of chondrocyte dedifferentiation.

Keywords: Long noncoding RNA, dedifferentiation, chondrocyte, autologous chondrocyte implantation, osteoarthritis, microRNA

Background

Articular cartilage injury and degeneration are few of the most common diseases worldwide, with their prevalence increasing with patients' age (1,2). There are no blood vessels or nerves in articular cartilage and its nutrition mainly depends on diffusion mechanism from the synovial fluid. Therefore, once articular cartilage is damaged, it is difficult to self-repair. Osteoarthritis (OA) may occur if the cartilage is not repaired in time with typical pathological features including chondrocyte degeneration, extracellular matrix degradation, and osteogenesis (3). OA can occur in multiple joints and causes clinical symptoms such as joint pain, swelling, stiffness, deformity, and limited movement (4-6). Although symptoms can be relieved by medication in the early stages of OA (7,8), patients may need surgical treatment (9) such as artificial joint replacement. There is still a lack of effective treatment for cartilage injury and defects. Progress has been made in microfractures and autologous cartilage grafts; however, several disadvantages remain such as limited cartilage source, small repair area, and microfractures that often cause fibrocartilage repair (10,11).

Autologous chondrocyte implantation (ACI) is an effective method for the treatment

of chronic articular cartilage defect in recent years, which may aid in rehabilitation of patients with cartilage defects. ACI technology was first established in 1994 and has been developed to the third generation, namely matrix-associated ACI (MACI) (12). ACI technology involves obtaining a small piece of tissue with autologous hyaline chondrocytes from healthy sites, isolating and subculturing sufficient number of hyaline chondrocytes in vitro, and implanting the cells to the site of cartilage defect, thus repairing the defect (13). However, human hyaline chondrocytes often undergo dedifferentiation in vitro (14). Dedifferentiation refers to the process in which well-differentiated mature cells gradually lose their differentiated phenotype and transform into undifferentiated cells (15). It is reported that the dedifferentiation of human hyaline chondrocytes occurs during passage culture in vitro. The expression of hyaline chondrocyte marker genes such as *COL2* (type II collagen) and *SOX*-9 (SRY-Box transcription factor 9) are downregulated. Conversely, the expression of fibrosis chondrocyte marker genes such as *COL1* (type I collagen) is upregulated (16,17). Due to dedifferentiation, it is impossible to obtain enough hyaline chondrocytes. There are two methods to make dedifferentiated chondrocytes undergo redifferentiation. One is to add a variety of cytokines, such as TGF-β1, BMP-2, and growth differentiation factor 5 (GDF-5) (18-20). The other method is to employ three-dimensional culture, such as pellet, suspension, and gel cultures (21,22). In addition, some studies have demonstrated a “dedifferentiated-like” phenotype that might also contribute to chondrocyte degeneration. However, limited data about mechanism of dedifferentiation are available. Therefore, clarifying the mechanism of

dedifferentiation is important for the development of ACI technology (23,24).

Long non-coding RNA (lncRNA) refers to non-coding RNA with a length of more than 200 nucleotides. It has a regulatory role in a variety of physiological and pathological processes. Many lncRNAs were identified in cartilage, such as lncRNA-HIT and ROCR (25). In addition, several lines of evidence suggest that lncRNAs play a role in OA. It was revealed that lncRNA-GAS5 contributes to the pathogenesis of OA through negative regulation of miRNA (miR)-21 (26). It was also identified that lncRNA-MEG3 inhibits angiogenesis in OA (27). TMSB4 pseudogene lncRNA promotes cartilage degeneration in human OA as competing endogenous RNA (ceRNA; 28). However, the role of lncRNAs in the process of human hyaline chondrocyte dedifferentiation remains unknown.

In this study, we identified the expression profiles of lncRNAs during human hyaline chondrocyte dedifferentiation. Among them, we selected a typical lncRNA (AP001505.9) to study its specific mechanism in chondrocyte dedifferentiation, thereby laying a foundation for further study on the pathogenesis of dedifferentiation and OA.

METHODS

Articular cartilage donors

Human cartilage tissues were harvested from donors immediately after death or trauma (n = 3; age = 39, 55, 67 years; 2 male and 1 female). All tissues were

examined by safranin O staining and graded according to a modified Mankin scale. The tissues with scores < 2 were considered normal hyaline cartilage. All three patients or their families included in the study signed informed consent. This study was approved by the Clinical Ethics Committee of China-Japan Union Hospital of Jilin University.

Passage culture of chondrocytes in vitro

Cartilage tissues were cut into small pieces and incubated overnight in Dulbecco's modified Eagle's medium (DMEM; HyClone, SH30023.01) containing 1 mg/mL type II collagenase (Sigma, YDM2138) at 37°C and 5% CO_2. Primary chondrocytes were cultured in DMEM supplemented with 10% fetal bovine serum (FBS; TransGen Biotech Co. Ltd., Beijing, China, FS201-02) and 1% penicillin-streptomycin (Invitrogen, USA, 15140122) at a density of 25,000 cells/cm^2. The culture medium was changed every two days. When more than 80% chondrocytes fused, cells were passaged with 0.25% trypsin-EDTA (Gibco, USA, 25200056) until P5, and the P1 and P5 chondrocytes were selected for further experiments.

Real-time quantitative PCR (qPCR)

TRIzol Reagent (Invitrogen, 15596026) was used to extract total RNA according to manufacturer's instructions. One-Step gDNA Removal (TransGen) and cDNA Synthesis SuperMix (TransGen, AT311-03) were used for mRNA and lncRNA real-time qPCR following the manufacturer's instructions. All-in-One First-Strand cDNA Synthesis Kit (GeneCopoeia, USA, QP014) was used for synthesizing cDNA

for microRNA real-time qPCR following the manufacturer's instructions.

We used Applied Biosystems 7300 Plus Real-time PCR System for real-time qPCR detection. ChamQ Universal SYBR qPCR Master Mix (Vazyme, Nanjing, China, Q711) kit was used for mRNA and lncRNA real-time qPCR. The primers of target genes (Table S1) were purchased from Sangon Biotech Co. Ltd, Shanghai, China. All-in-One miRNA qRT-PCR Reagent Kit (GeneCopoeia, QP002) was used for real-time qPCR of miRNAs. The primers for miRNA used are presented in Table S2. The reaction system was set up as per the instructions of the kit manufacturer. *GAPDH* (glyceraldehyde-3-phosphate dehydrogenase), *β-actin* and *U6* were used as internal references and relative quantitative statistical analysis was performed using the $2^{-\triangle\triangle Ct}$ method.

Western blotting

Chrondrocytes total protein was extracted with RIPA (radioimmunoprecipitation assay) Lysis Buffer (Beyotime, P0013D) containing 1% protease inhibitor phenylmethylsulfonyl fluoride (Beyotime, P1011). The protein sample (10–30 mg) was separated using 10% PAGE and transferred to polyvinylidene difluoride membrane. After elution, the target antibodies were added: anti-COL2 (Rockland, ab17771), anti-COL1 (Abcam, ab34710), anti-SOX-9 (Millipore, AB5535), anti-β-actin (CMC TAG), and anti-GAPDH (CMC TAG, AT0002) and allowed to incubate overnight. The goat anti-rabbit/anti-mouse IgG (Amersham Pharmacia Biotech Ltd.) was labeled with horseradish peroxidase (ELISA) and the

148 hypersensitive ECL (enhanced chemiluminescence) kit was used to develop the color
149 in the gel imager. ImageJ software was used to analyze and count the gray value of
150 the electrophoresis image after color rendering.

151 **Immunofluorescence**

152 Cells were inoculated into 24-well plates at a density of 5×10^4/well. After 24 h of
153 incubation at 5% CO_2 and 37°C, the cells were fixed with 4% paraformaldehyde,
154 perforated with 0.1% Triton X-100, and incubated with 10% goat serum for 1 h. The
155 primary antibodies anti-COL2 (Rockland), anti-COL1 (Abcam), and anti-SOX-9
156 (Millipore) were added and incubated at 4°C overnight. The next day, fluorescent
157 antibodies were used to block the cells for 1 h, and Hoechst 33342 (Beyotime) was
158 used to stain the nuclei. The results were observed under inverted phase contrast
159 fluorescence microscope.

160 **Microarray analyses**

161 Arraystar Human LncRNA Microarray V4.0 was used to detect 40,173 lncRNAs and
162 20,730 coding transcripts. The hybridized arrays were washed, fixed, and scanned
163 using the Agilent DNA Microarray Scanner System (part number G2505C). Agilent
164 Feature Extraction software (version 11.0.1.1) was used to analyze the acquired array
165 images.

166 **The coding-non-coding gene co-expression (CNC) network**

167 CNC network was constructed based on the correlation analysis between the
168 differentially expressed lncRNAs and mRNAs. LncRNAs and mRNAs with Pearson

correlation coefficients not less than 0.99 were selected to draw the network using open source bioinformatics software Cytoscape (Institute of Systems Biology in Seattle).

CeRNA analyses

To identify potential targets of miRNAs, they are predicted with miRNA target prediction software based on TargetScan and miRanda. By merging commonly targeted miRNAs, we constructed a ceRNA network.

Chondrocyte redifferentiation

P5 chondrocytes were inoculated in a 15 mL centrifugal tube at a density of 2×10^5 cells and cultured with 0.5 mL cartilage induction medium (DMEM High Glucose; TransGen Biotech Co. Ltd., Beijing, China) containing 0.4% sodium pyruvate, 0.1% proline, 0.25% vitamin C, 0.1% TGF-β3, 1% ITS (insulin-transferrin-selenium), 0.2% dexamethasone, and 1% penicillin-streptomycin double antibody. The culture medium was replaced every two days and terminated on day 7.

Histological staining

Hematoxylin-eosin (HE) staining: After 48 h of fixation, the cartilage pellets were embedded in paraffin and sliced. After xylene dewaxing and washing, the sections were soaked in hematoxylin solution for 5 min, differentiated in 1% hydrochloric acid-alcohol mixture, dipped in weak aqueous ammonia, stained in eosin dye solution for 15 min, dehydrated using gradient alcohol, and sealed.

Saffron O staining: After dewaxing and washing, sections were stained in hematoxylin solution for 10 min, washed, differentiated in 1% acetic acid solution, stained in saffron O dyeing solution for 10 min, dehydrated with gradient alcohol, and sealed.

Alcian blue staining: After dewaxing and washing, the sections were stained in Alcian blue for 30 min, washed in water for 5 min, stained in nuclear fixing red dye for 10 min, washed, dehydrated with gradient alcohol, transparentized with xylene, and sealed.

Immunohistochemistry

After dewaxing and washing, the sections were incubated in peroxidase blocking solution. After incubation with normal non-immune animal serum, the following primary antibodies were added: anti-COL2 (Rockland), anti-COL1 (Abcam), and anti-SOX-9 (Millipore), and incubated overnight. After washing, the sections were incubated with goat anti-mouse/rabbit IgG labeled with biotin for 10 min. After PBS washing, *Streptomyces* antibiotic-peroxidase solution was added to the sections and incubated for 10 min. Sections were stained with DAB (3,3'-diaminobenzidine) reagent kit, as per the instructions of the manufacturer. The sections were re-dyed with hematoxylin solution, dehydrated with gradient alcohol, transparentized with xylene, and sealed with neutral gum. The images were observed and photographed using an inverted microscope (Olympus).

Lentiviral transfection

P5 human chondrocytes were inoculated into a 24-well plate at a density of 5 × 10^4/well and cultured in culture medium mentioned above. After 24 h, it was replaced with viral transfection solution (Genechem Co. Ltd, China). Cells were transduced with lentiviruses carrying AP001505.9 (Genechem Co. Ltd, China) at multiplicity of infection (MOI) = 75. Transduced chondrocytes were subcultured after 80% confluency.

FISH

Cells, seeded at 5 × 10^4/well in 24-well plates, were incubated for 24 h, fixed with 4% paraformaldehyde, and permeated with 0.5% Triton X-100. LncRNA Probe Mix (RiboBio) and Fluorescent In Situ Hybridization Kit (RiboBio) were used for detection following the manufacturer's instructions. U6 and 18S were used as internal references.

Double luciferase labeling

293T cells in logarithmic growth phase were seeded at 1.5 × 10^4/well in 96-well plates and cultured in 37°C for 24 h. The transfection concentration was 50 nM, and the plasmid concentration was 50 ng/pore. Each group had three pores. After 48 h of transfection, the culture medium was discarded, and the fluorescence value was determined by adding 1× PBS and luciferase substrate with 35 μL/pore, and oscillating for 10 min. The fluorescence value was determined by fluorescence photometer after adding 30 μL stop reagent and oscillating for 10 min.

miR-495 mimic transfection

231 Cells were inoculated into a 24-well plate at a density of 5×10^4/well. The cell density
232 reached 30%–50% at the time of transfection. The cells were transfected with
233 Transfection Reagent (RiboBio) and miR-495 Mimic (RiboBio) according to the
234 manufacturer's instructions. After 72 h, RNA and protein were extracted for real-time
235 qPCR and western blotting, respectively.

236 **Subcutaneous transplantation in nude mice**

237 The BALB/C A-nu (nude) mice (male, 4–5 weeks old, about 15 g) used in the
238 experiment were purchased from Beijing HFK BioScience Co. Ltd. All the animal
239 experiments were approved by the Animal Experiment Ethics Committee of the Basic
240 Medical College of Jilin University (#202003). Intraperitoneal injection of 0.8%
241 pentobarbital sodium was used for anesthesia. Using 100 μL porcine fibrin sealant kit
242 (Guangzhou Bioseal Biotech Co. Ltd.) as scaffold material, the P5 chondrocytes
243 transfected with LV-AP001505.9 (1×10^6) were transplanted into the left dorsal
244 subcutaneous tissue of ten male nude mice. The same number of chondrocytes
245 transfected with negative control (NC)-lentivirus were transplanted into the right
246 dorsal subcutaneous tissue of the same mouse. One month later, all the mice were
247 sacrificed, and the samples were used for histological and immunohistochemical
248 analysis.

249 **Statistical analysis**

250 SPSS19.0 software was used to analyze the data in this study. The measurement data
251 were tested using *t*-test and counting data using chi-squared test. Variance analysis

was performed for all data, and Fisher's minimum significant difference test was applied where appropriate. In all experiments, the data are expressed in the form of mean ± SD (standard deviation), and $P < 0.05$ was considered significant.

Results

Human hyaline chondrocytes underwent dedifferentiation during passage culture

During passage culture, the shape of human hyaline chondrocytes gradually changed from polygonal or near-circular to flat and long and spindly (Figure 1a). Compared with P1 chondrocytes, the expression of COL2A1 and SOX-9 in P5 chondrocytes was significantly downregulated, while the expression of COL1A1 was significantly upregulated (Figure 1b). Levels of COL2 and SOX-9 proteins in P5 chondrocytes were significantly lower than those in P1 chondrocytes, while the levels of COL1 in P5 chondrocytes were significantly higher than those in P1 chondrocytes (Figures 1c-g). These results suggest that dedifferentiation of human hyaline chondrocytes occurs during passage culture in vitro.

Expression profile of lncRNAs in human chondrocyte dedifferentiation

Microarray analysis of P1 and P5 human chondrocytes revealed that 334 lncRNAs were upregulated and 381 lncRNAs were downregulated in P5 human chondrocytes compared with P1 human chondrocytes. Among these, the expression of 49 lncRNAs in P5 chondrocytes was more than twice of that in P1 chondrocytes, while the expression of 83 lncRNAs in P5 chondrocytes was more than two-fold

lower. Seven lncRNAs were upregulated more than five-fold, and 13 lncRNAs were downregulated more than five-fold (Figures 2a-c). The top 20 lncRNAs with the greatest change in expression are shown in Table S3. These results indicate that the number of downregulated lncRNAs was higher than the upregulated lncRNAs, suggesting that these lncRNAs may play a regulatory role in the process of human hyaline chondrocyte dedifferentiation in vitro.

We also detected differentially expressed mRNAs during dedifferentiation of human chondrocytes. The expression of 51 genes in P5 human chondrocytes was significantly upregulated by more than two-fold, and the expression of 191 genes was significantly downregulated by more than two-fold. Two of these were upregulated more than five-fold, 42 were downregulated more than five-fold (Figures 2d-f), and the top ten altered mRNAs are listed in Table S4. *COL9A1*, a marker gene of chondrocytes, was downregulated by approximately 25-fold in P5 chondrocytes. These differentially expressed genes might be involved in the process of regulating dedifferentiation.

Gene ontology (GO) analysis results suggest that differentially expressed genes may lead to dedifferentiation by regulating the expression and activity of biological processes, cellular components, and molecular functions (Figures 2g, h). Pathway analysis revealed downregulated pathways including DNA replication, nitrogen metabolism, Hippo signaling, and butyrate metabolism during the dedifferentiation of human chondrocytes (Figure 2i). The upregulated pathways include P53 signaling, purine metabolism, ErbB signaling, HIF1 signaling, and pyrimidine metabolism

(Figure 2j). Therefore, we hypothesize that differentially expressed lncRNAs may directly or indirectly regulate the expression of target genes, thereby altering the expression of downstream signaling pathways, ultimately leading to human chondrocyte dedifferentiation in vitro.

Expression of selected lncRNAs validated by real-time qPCR

We selected ten lncRNAs that met the following conditions: (1) Fold change and *P* value: the lncRNAs should have higher fold change and smaller *P* value; (2) Raw intensity: the raw intensity of the lncRNAs should more than 200; (3) RNA length: the length of the lncRNAs should generally less than 2000 bp to facilitate the follow-up function research; (4) Relationship: sense-overlap lncRNAs were avoided (5) Source: RefSeq, UCSC Known Gene, or GENCODE for lncRNAs. We performed real-time qPCR for these selected lncRNAs and several mRNAs that showed significant change in expression to validate the results of microarray analysis. Except for G062245 (T268788), the qPCR results of all selected lncRNAs were consistent with those of microarray analysis. The expression of LINC01021 (NR_038848) and GS1-600G8.5 (ENST00000412485) have the most fold change in upregulating lncRNAs (Figure 3a). The expression of AP001505.9 (ENST00000569966, LINC00165) and LINC00162 (NR_024089) have the most fold change in downregulating lncRNAs (Figure 3b). The expression of selected mRNAs in real-time qPCR was consistent with microarray analysis (Figure 3c, d). These results demonstrate that microarray analysis results were accurate and thus, can be used for further experiments. Next, we analyzed the gene co-expression network of AP001505.9, LINC00162, LINC01021, and

GS1-600G8.5 and explored potential target genes for future research (Figure 3e).

LncRNA expression reversed during chondrocyte redifferentiation

Dedifferentiated chondrocytes can be redifferentiated using pellet culture (21). In order to further clarify whether the expression of lncRNAs in chondrocyte redifferentiation can be reversed, P5 chondrocytes were cultured in pellet culture in vitro. Firstly, we found that chondrocytes after pellet culture had typical hyaline chondrocyte characteristics and the extracellular matrix was increased significantly after pellet culture (Figures 4a-c). The expression of COL1 was significantly downregulated, while the expression of COL2 and SOX-9 was significantly upregulated (Figure 4d-g). This suggests that dedifferentiated P5 chondrocytes can be redifferentiated using pellet culture. Then, we further examined the expression of previously selected lncRNAs during redifferentiation. Real-time qPCR analysis showed that AP001505.9 and LINC00162 were upregulated, while LINC01021 and GS1-600G8.5 were downregulated (Figures 4h and 4i). This suggests that the expression of lncRNAs was reversed during chondrocyte redifferentiation.

AP001505.9 promotes the maintenance of human chondrocyte phenotype and inhibits dedifferentiation

To further analyze the effects of AP001505.9, we transfected lentiviruses carrying AP001505.9 into P5 chondrocytes to overexpress AP001505.9. Fluorescence microscopy confirmed 80% transfection efficiency (Figure 5a). Real-time qPCR showed that the expression of AP001505.9 was upregulated approximately 20-fold

qPCR (Figure 5b), confirming successful lentiviral transfection of human chondrocytes. Overexpression of AP001505.9 led to significant upregulation of expression of SOX-9 at both genetic and protein levels, while significantly downregulating COL1 (Figure 5c-h). These results suggest that overexpression of AP001505.9 promoted the maintenance of hyaline chondrocyte phenotype and inhibited dedifferentiation in chondrocytes.

Next, we explored the role of AP001505.9 in vivo using a subcutaneous transplantation mice model. Compared to the control group, the pellet formed by transplantation of overexpressed AP001505.9 chondrocytes showed typical cartilage morphology and increased extracellular matrix content (Figure 6a, e). The expression of COL2 and SOX-9 was significantly higher than that of the control group, while the expression of COL1 was significantly lower than that of the control group (Figure 6 b-d, f-h). The results showed that AP001505.9 also promoted the maintenance of chondrocyte phenotype and inhibited dedifferentiation in vivo.

AP001505.9 promoted SOX-9 expression and inhibited COL1 expression, thus inhibiting dedifferentiation

We demonstrated that AP001505.9 was mainly located in cytoplasm (Figure 7a) and thus assessed potential mechanism of AP001505.9-inhibited hyaline chondrocyte dedifferentiation. CeRNA analysis showed that AP001505.9 may regulate SOX-9 expression by inhibiting the expression of four miRNAs: hsa-miR-495-3p, hsa-miR-518a-5p, hsa-miR-5688, and hsa-miR-6887-3p (Figure 7b). Further,

real-time qPCR results showed that the expression of miR-495-3p and miR-518a-5p was significantly upregulated during dedifferentiation of human chondrocytes, while the expression of miR-5688 was significantly downregulated (Figure 7c). The expression of miR-495-3p and miR-518a-5p was significantly downregulated in the process of regeneration (Figure 7d). Overexpression of AP001505.9 inhibited the expression of miR-495-3p but had no significant impact on miR-518a-5p and miR-5688 (Figure 7e). These results suggest that AP001505.9 may promote SOX-9 expression by inhibiting the expression of miR-495-3p.

SOX-9 was previously identified as a target of miR-495-3p (29). Therefore, we established chondrocytes overexpressing miR-495 using miR-495-3p mimics to probe the regulation of SOX-9. The expression of miR-495-3p was upregulated nearly 20-fold after transfection (Figure 7f). However, AP001505.9 was significantly downregulated (Figure 7g). Also, expression of SOX-9 was significantly downregulated at both mRNA and protein levels (Figure 7h-j). To verify whether AP001505.9 was directly regulated by miR-495-3p, we screened for potential binding sites of miR-495-3p on AP001505.9 (Figure 7k) and designed a double luciferase experiment. Interestingly, reported fluorescence of wild-type vectors of AP001505.9 was not significantly downregulated by miR-495-3p mimic, suggesting the possibility of an indirect co-regulatory mechanism (Figure 7l). Based on these results, we conclude that overexpression of AP001505.9 promoted the expression of SOX-9 and inhibited the expression of COL1, thus inhibiting human chondrocyte dedifferentiation.

Discussion

Articular cartilage injury and degeneration brings serious economic burden to their families and the society (30). The rise of ACI technology has brought hope for rehabilitation of these patients and is currently considered to be the best treatment for cartilage injury (31). Although stem cells such as bone marrow mesenchymal stem cells, embryonic stem cells, pluripotent stem cells, and umbilical cord blood stem cells can be used as seed cells, the use of stem cells has many problems, such as ethical factors, differentiation instability, and cancer risk (32). Therefore, human autologous chondrocytes are the most suitable seed cells and have been applied in ACI technology. However, their application is limited due to dedifferentiation in subculture, characterized by the absence of hyaline chondrocyte phenotype and the enhancement of fibrochondrocyte phenotype, conditions that are very similar to the formation of OA.

LncRNAs have been a research hotspot in recent years and have been identified to play an important role in the differentiation of cartilage and the formation of OA (26-28). In this study, the expression profiles of lncRNAs during the process of dedifferentiation of in vitro human hyaline chondrocytes were obtained for the first time. A large number of differentially expressed lncRNAs were identified. We hypothesize that AP001505.9 and LINC00162, which were downregulated during dedifferentiation, may play a role in inhibiting chondrocyte dedifferentiation. LINC01021 and GS1-600G8.5 were identified to promote chondrocyte dedifferentiation. We selected pellet culture to make the dedifferentiated chondrocytes

redifferentiate. In the process of redifferentiation, the expression of lncRNAs was reversed, with the upregulation of AP001505.9 being nearly three-fold. In view of these four lncRNAs regulating dedifferentiation, we first studied the role of AP001505.9 in chondrocyte dedifferentiation and its mechanism.

Pathway analysis showed that there were significant changes in the expression of signaling pathways during dedifferentiation. DNA replication, nitrogen metabolism, Hippo signaling, and butyrate metabolism pathways were significantly downregulated, while P53 signaling, purine metabolism, ErbB signaling, HIF1 signaling, and pyrimidine metabolism pathways were significantly upregulated. Studies have shown that these signaling pathways are also involved in the formation and progression of OA, such as DNA replication (33), Hippo signaling (34), p53 signaling pathway, (35) and HIF1 pathway (36). These results showed that the process of dedifferentiation is very similar to the pathogenesis of OA.

An important role of lncRNA is to act as a ceRNA to inhibit the expression of miRNAs, thus promoting the expression of target genes (37, 38). SOX-9 is an HMG-box (high mobility group box) transcription factor that plays an essential role in chondrocyte development by directing the expression of chondrocyte-specific genes (38). Studies have shown that SOX-9 can promote the expression of chondrocyte marker genes and inhibit dedifferentiation (39). However, when SOX-9 was knocked out, the expression of chondrocyte marker genes was found to be significantly downregulated (40). Many microRNAs (miRNAs) in chondrocytes can regulate the expression of SOX-9, thus promoting the pathogenesis of OA, such as miR-145 (41),

miR-495 (29), and miR-1247 (42). In our ceRNA analysis, we found that AP001505.9 may regulate SOX-9 expression through four miRNAs; miR-495-3p, miR-518a-5p, miR-5668, and miR-6887. We detected these miRNAs separately and found that the expression of miR-495-3p was significantly upregulated during dedifferentiation and downregulated during redifferentiation in pellet culture. Overexpression of AP001505.9 significantly decreased the expression of miR-495-3p. Luciferase assay indicated that AP001505.9 cannot directly bind to miR-495-3p, therefore, AP001505.9 may regulate the expression of miR-495-3p through other indirect ways. AP001505.9 promoted the expression of SOX-9 by regulating miR-495-3p, ultimately promoting the maintenance of chondrocyte phenotype and inhibiting dedifferentiation. This was also verified by in vivo experiments. That is, AP001505.9/miR-495-3p/SOX-9 axis promoted phenotype maintenance and suppressed the dedifferentiation of chondrocytes.

The limitations of this study include the lack of description of the role of AP001505.9 in animal model of cartilage injury. It is very difficult to obtain hyaline cartilage in clinical settings; therefore, it is very important to carry out in vivo animal experiments. In the future, we will study whether AP001505.9 can maintain chondrocyte phenotype and inhibit dedifferentiation in animal models of cartilage injury. We will also study the cartilage in OA to investigate the expression profiles of lncRNAs in OA patients, as the process of dedifferentiation is similar to the process of OA.

In conclusion, this study, for the first time, elucidated the expression and

characteristics of lncRNAs in the process of human hyaline chondrocyte dedifferentiation in vitro. We identified that AP001505.9 can inhibit dedifferentiation and promote the maintenance of chondrocyte phenotype by regulating SOX-9. This discovery paves the way for further study on the mechanism of dedifferentiation and the treatment of OA. Further functional studies of lncRNAs are required to explore the underlying regulatory mechanisms.

Declarations

Ethics approval and consent to participate

All three patients or their families included in the study signed informed consent. This study was approved by the Clinical Ethics Committee of China-Japan Union Hospital of Jilin University.

Consent for publication

Not applicable.

Availability of data and materials

The accession number for the array data reported in this paper is available at Gene Expression Omnibus: GSE145817.

Competing interests

The authors declare that they have no competing interests.

Funding

This work was supported by the National Natural Science Foundation of China (81970547) and the Fundamental Research Funds for the Central Universities, Jilin University.

Authors' contributions

LC, YL, and GC conceived and designed the study. LC conducted the in vivo and in vitro experiments, with help from JX and SL. YZ and XL performed statistical analysis. DS and LZ performed immunohistochemistry. LC wrote the manuscript with input from YZ, YL, and GC.

Acknowledgments

The authors wish to acknowledge support from Guangzhou RiboBio Co., Ltd for double luciferase labeling experiment, KangChen Bio-tech Co., Ltd for microarray and ceRNA analysis and Shanghai GeneChem Co. Ltd. for designing the lentiviruses. We would like to thank Editage (www.editage.cn) for English language editing.

Authors' information

LC, PhD, jluchenlin@163.com; JX, PhD, 1191781943@qq.com; Sl, PhD, lvshuang@jlu.edu.cn; YZ, MD, 315229028@qq.com; DS, PhD, sunparrow@126.com; YZ, PhD, 1753826287@qq.com; XL, PhD, 565373780@qq.com; LZ, MD, jluchenlin@yeah.net, GChi, PhD, guangfan130@jlu.edu.cn; YL,PhD, ylli@jlu.edu.cn.

REFERENCES

1. Chung JY, Song M, Ha CW, Kim JA, Lee CH, Park YB. Comparison of articular

cartilage repair with different hydrogel-human umbilical cord blood-derived mesenchymal stem cell composites in a rat model. Stem Cell Res Ther 2014;5:39. doi:10.1186/scrt427.

2. Zhang C, Wang P, Jiang P, Lv Y, Dong C, Dai X, Tan L, Wang Z. Upregulation of lncRNA HOTAIR contributes to IL-1β-induced MMP overexpression and chondrocytes apoptosis in temporomandibular joint osteoarthritis. Gene 2016; 586: 248-253. doi:10.1016/j.gene.2016.04.016.

3. Pearson MJ, Philp AM, Heward JA, Roux BT, Walsh DA, Davis ET, Lindsay MA, Jones SW. Long Intergenic Noncoding RNAs Mediate the Human Chondrocyte Inflammatory Response and Are Differentially Expressed in Osteoarthritis Cartilage. Arthritis Rheumatol 2016;68:845–856. doi:10.1002/art.39520.

4. Song J, Kim D, Lee CH, Lee MS, Chun CH, Jin EJ. MicroRNA-488 regulates zinc transporter SLC39A8/ZIP8 during pathogenesis of osteoarthritis. J Biomed Sci 2013;20:31. Published 2013 May 20. doi:10.1186/1423-0127-20-31.

5. Jiang SD, Lu J, Deng ZH, Li YS, Lei GH. Long noncoding RNAs in osteoarthritis [review]. Joint Bone Spine 2017; 84: 553-556. doi: 10.1016/j.jbspin.2016.09.006.

6. Ko JY, Kim KI, Park S, Im GI. In vitro chondrogenesis and in vivo repair of osteochondral defect with human induced pluripotent stem cells. Biomaterials 2014;35:3571–3581. doi:10.1016/j.biomaterials.2014.01.009.

7. Funayama A, Niki Y, Matsumoto H, Maeno S, Yatabe T, Morioka H, Yanagimoto S, Taguchi T, Tanaka J, Toyama Y. Repair of full-thickness articular cartilage defects

using injectable type II collagen gel embedded with cultured chondrocytes in a rabbit mode. J Orthop Sci 2008;13:225 – 232. doi:10.1007/s00776-008-1220-z.

8. Jiménez G, López-Ruiz E, Kwiatkowski W, Montañez E, Arrebola F, Carrillo E, Gray PC. Activin A/BMP2 chimera AB235 drives efficient redifferentiation of long term cultured autologous chondrocytes. Sci Rep. 2015;5:16400. Published 2015 Nov 13. doi:10.1038/srep16400.

9. Broyles JE, O'Brien MA, Stagg MP. Microdrilling Surgery Augmented With Intra-articular Bone Marrow Aspirate Concentrate, Platelet-Rich Plasma, and Hyaluronic Acid: A Technique for Cartilage Repair in the Knee. Arthrosc Tech. 2017;6:e201 – e206. Published 2017 Feb 13. doi:10.1016/j.eats.2016.09.024.

10. Frehner F, Benthien JP. Microfracture: State of the Art in Cartilage Surgery? [review]. Cartilage. 2018;9:339 – 345. doi:10.1177/1947603517700956.

11. Haraguchi N, Ota K, Nishida N, Ozeki T, Yoshida T, Tsutaya A. T1ρ mapping of articular cartilage grafts after autologous osteochondral transplantation for osteochondral lesions of the talus: A longitudinal evaluation. J Magn Reson Imaging. 2018;48:398 – 403. doi:10.1002/jmri.25962.

12. Hoburg A, Löer I, Körsmeier K, Siebold R, Niemeyer P, Fickert S, Ruhnau K. Matrix-Associated Autologous Chondrocyte Implantation Is an Effective Treatment at Midterm Follow-up in Adolescents and Young Adults. Orthop J Sports Med 2019;7:2325967119841077. Published 2019 Apr 25. doi:10.1177/2325967119841077.

13. Ma B, Leijten JC, Wu L, Kip M, van Blitterswijk CA, Post JN, Karperien M.

528 Gene expression profiling of dedifferentiated human articular chondrocytes in
529 monolayer culture. Osteoarthritis Cartilage 2013;21:599 – 603.
530 doi:10.1016/j.joca.2013.01.014.

531 14. Dong N, Wang W, Tian J, Xie Z, Lv B, Dai J, Jiang R, Huang D, and Fang S, Tian
532 J., et al. MicroRNA-182 prevents vascular smooth muscle cell dedifferentiation via
533 FGF9/PDGFR β signaling. Int J Mol Med 2017;39:791 – 798.
534 doi:10.3892/ijmm.2017.2905.

535 15. Wuest SL, Caliò M, Wernas T, Tanner S, Giger-Lange C, Wyss F, Ille F,
536 Gantenbein B, Egli M. Influence of Mechanical Unloading on Articular Chondrocyte
537 Dedifferentiation. Int J Mol Sci 2018;19:1289. Published 2018 Apr 25.
538 doi:10.3390/ijms19051289.

539 16. Sliogeryte K, Botto L, Lee DA, Knight MM. Chondrocyte dedifferentiation
540 increases cell stiffness by strengthening membrane-actin adhesion. Osteoarthritis
541 Cartilage 2016;24:912 – 920. doi:10.1016/j.joca.2015.12.007.

542 17. Duan L, Liang Y, Ma B, Zhu W, Wang D. Epigenetic regulation in chondrocyte
543 phenotype maintenance for cell-based cartilage repair. Am J Transl Res 2015;7:2127
544 – 2140. Published 2015 Nov 15.

545 18. Miyatake K, Iwasa K, McNary SM, Peng G, Reddi AH. Modulation of Superficial
546 Zone Protein/Lubricin/PRG4 by Kartogenin and Transforming Growth Factor- β 1 in
547 Surface Zone Chondrocytes in Bovine Articular Cartilage. Cartilage 2016;7:388 – 397.
548 doi:10.1177/1947603516630789.

549 19. Mimura T, Imai S, Okumura N, Li L, Nishizawa K, Araki S, Ueba H, Kubo M,
550 Mori K, Matsusue Y. Spatiotemporal control of proliferation and differentiation of
551 bone marrow-derived mesenchymal stem cells recruited using collagen hydrogel for
552 repair of articular cartilage defects. J Biomed Mater Res B Appl Biomater
553 2011;98:360 – 368. doi:10.1002/jbm.b.31859.

554 20. Murphy MK, Huey DJ, Hu JC, Athanasiou KA. TGF-β1, GDF-5, and BMP-2
555 stimulation induces chondrogenesis in expanded human articular chondrocytes and
556 marrow-derived stromal cells. Stem Cells 2015;33:762 – 773. doi:10.1002/stem.1890.

557 21. Nguyen LH, Kudva AK, Saxena NS, Roy K. Engineering articular cartilage with
558 spatially-varying matrix composition and mechanical properties from a single stem
559 cell population using a multi-layered hydrogel. Biomaterials. 2011;32:6946 – 6952.
560 doi:10.1016/j.biomaterials.2011.06.014.

561 22. Lee J, Choi WI, Tae G, Kim YH, Kang SS, Kim SE, Kim SH, Jung Y, and Kim
562 SH. Enhanced regeneration of the ligament-bone interface using a poly (L-lactide-co-
563 ε-caprolactone) scaffold with local delivery of cells/BMP-2 using a heparin-based
564 hydrogel. Acta Biomater 2011;7:244 – 257. doi:10.1016/j.actbio.2010.08.017.

565 23. Charlier E, Deroyer C, Ciregia F, Malaise O, Neuville S, Plener Z, Malaise M, de
566 Seny D. Chondrocyte dedifferentiation and osteoarthritis (OA) [review]. Biochemical
567 Pharmacology 2019; 165, 49 – 65.

568 24. Speichert S, Molotkov N, El Bagdadi K, Meurer A, Zaucke F, Jenei-Lanzl Z. Role
569 of Norepinephrine in IL-1 β -Induced Chondrocyte Dedifferentiation under Physioxia.

570 Int J Mol Sci 2019;20:1212. Published 2019 Mar 11. doi:10.3390/ijms20051212.

571 25. Barter MJ, Gomez R, Hyatt S, Cheung K, Skelton AJ, Xu Y, Clark IM, Young DA.
572 The long non-coding RNA ROCR contributes to SOX9 expression and chondrogenic
573 differentiation of human mesenchymal stem cells. Development 2017;144:4510 –
574 4521. doi:10.1242/dev.152504.

575 26. Song J, Ahn C, Chun CH, Jin EJ. A long non-coding RNA, GAS5, plays a critical
576 role in the regulation of miR-21 during osteoarthritis. J Orthop Res 2014;32:1628 –
577 1635. doi:10.1002/jor.22718.

578 27. Su W, Xie W, Shang Q, Su B. The Long Noncoding RNA MEG3 Is
579 Downregulated and Inversely Associated with VEGF Levels in Osteoarthritis. Biomed
580 Res Int 2015;2015:356893. doi:10.1155/2015/356893.

581 28. Liu Q, Hu X, Zhang X, Dai L, Duan X, Zhou C, Ao Y. The TMSB4 Pseudogene
582 LncRNA Functions as a Competing Endogenous RNA to Promote Cartilage
583 Degradation in Human Osteoarthritis. Mol Ther 2016;24:1726 – 1733.
584 doi:10.1038/mt.2016.151.

585 29. Lee S, Yoon DS, Paik S, Lee KM, Jang Y, Lee JW. microRNA-495 inhibits
586 chondrogenic differentiation in human mesenchymal stem cells by targeting Sox9.
587 Stem Cells Dev. 2014;23:1798 – 1808. doi:10.1089/scd.2013.0609.

588 30. Wu KC, Chang YH, Liu HW, Ding DC. Transplanting human umbilical cord
589 mesenchymal stem cells and hyaluronate hydrogel repairs cartilage of osteoarthritis in
590 the minipig model. Ci Ji Yi Xue Za Zhi 2019; 31, 11-19. doi:

591 10.4103/tcmj.tcmj_87_18.

592 31. Kraeutler MJ, Belk JW, Purcell JM, McCarty EC. Microfracture Versus
593 Autologous Chondrocyte Implantation for Articular Cartilage Lesions in the Knee: A
594 Systematic Review of 5-Year Outcomes. Am J Sports Med. 2018;46:995 – 999.
595 doi:10.1177/0363546517701912.

596 32. Davies RL, Kuiper NJ. Regenerative Medicine: A Review of the Evolution of
597 Autologous Chondrocyte Implantation (ACI) Therapy. Bioengineering (Basel)
598 2019;6:22. Published 2019 Mar 13. doi:10.3390/bioengineering6010022.

599 33. De Leonardis F, Monti L, Gualeni B, Tenni R, Forlino A, Rossi A. Altered
600 signaling in the G1 phase deregulates chondrocyte growth in a mouse model with
601 proteoglycan undersulfation. J Cell Biochem 2014;115:1779 – 1786.
602 doi:10.1002/jcb.24844.

603 34. Ying J, Wang P, Zhang S, Xu T, Zhang L, Dong R, Xu S, Tong P, Wu C, Jin H.
604 Transforming growth factor-beta1 promotes articular cartilage repair through
605 canonical Smad and Hippo pathways in bone mesenchymal stem cells. Life Sci
606 2018;192:84 – 90. doi:10.1016/j.lfs.2017.11.028.

607 35. Yan S, Wang M, Zhao J, Zhang H, Zhou C, Jin L, Zhang Y, Qiu X, Ma B, and Fan
608 Q. MicroRNA-34a affects chondrocyte apoptosis and proliferation by targeting the
609 SIRT1/p53 signaling pathway during the pathogenesis of osteoarthritis. Int J Mol Med
610 2016;38:201 – 209. doi:10.3892/ijmm.2016.2618.

611 36. Miao H, Chen L, Hao L, Zhang X, Chen Y, Ruan Z, Liang H. Stearic acid induces

612 proinflammatory cytokine production partly through activation of lactate-HIF1 α
613 pathway in chondrocytes. Sci Rep 2015;5:13092. Published 2015 Aug 14.
614 doi:10.1038/srep13092.

615 37. Liu C, Ren S, Zhao S, Wang Y. LncRNA MALAT1/MiR-145 Adjusts IL-1 β
616 -Induced Chondrocytes Viability and Cartilage Matrix Degradation by Regulating
617 ADAMTS5 in Human Osteoarthritis. Yonsei Med J 2019;60:1081 – 1092.
618 doi:10.3349/ymj.2019.60.11.1081.

619 38. Mao G, Kang Y, Lin R, Hu S, Zhang Z, Li H, Liao W, Zhang Z. Long Non-coding
620 RNA HOTTIP Promotes CCL3 Expression and Induces Cartilage Degradation by
621 Sponging miR-455-3p. Front Cell Dev Biol 2019;7:161. Published 2019 Aug 23.
622 doi:10.3389/fcell.2019.00161.

623 39. Sekiya I, Tsuji K, Koopman P, Watanabe H, Yamada Y, Shinomiya K, Nifuji A,
624 Noda M. SOX9 enhances aggrecan gene promoter/enhancer activity and is
625 up-regulated by retinoic acid in a cartilage-derived cell line, TC6. J Biol Chem
626 2000;275:10738 – 10744. doi:10.1074/jbc.275.15.10738.

627 40. Akiyama H. Control of chondrogenesis by the transcription factor Sox9. Mod
628 Rheumatol 2008; 18: 213-9. doi: 10.1007/s10165-008-0048-x.

629 41. Martinez-Sanchez A, Dudek KA, Murphy CL. Regulation of Human Chondrocyte
630 Function through Direct Inhibition of Cartilage Master Regulator SOX9 by
631 MicroRNA-145(miRNA-145). J Biol Chem 2012; 287: 916 – 924.
632 doi:10.1074/jbc.M111.302430.

633 42. Martinez-Sanchez A, Murphy CL. MiR-1247 Functions by Targeting Cartilage
634 Transcription Factor SOX9. J Biol Chem 2013;288:30802 – 30814.
635 doi:10.1074/jbc.M113.496729.

636

637 **Figure legends:**

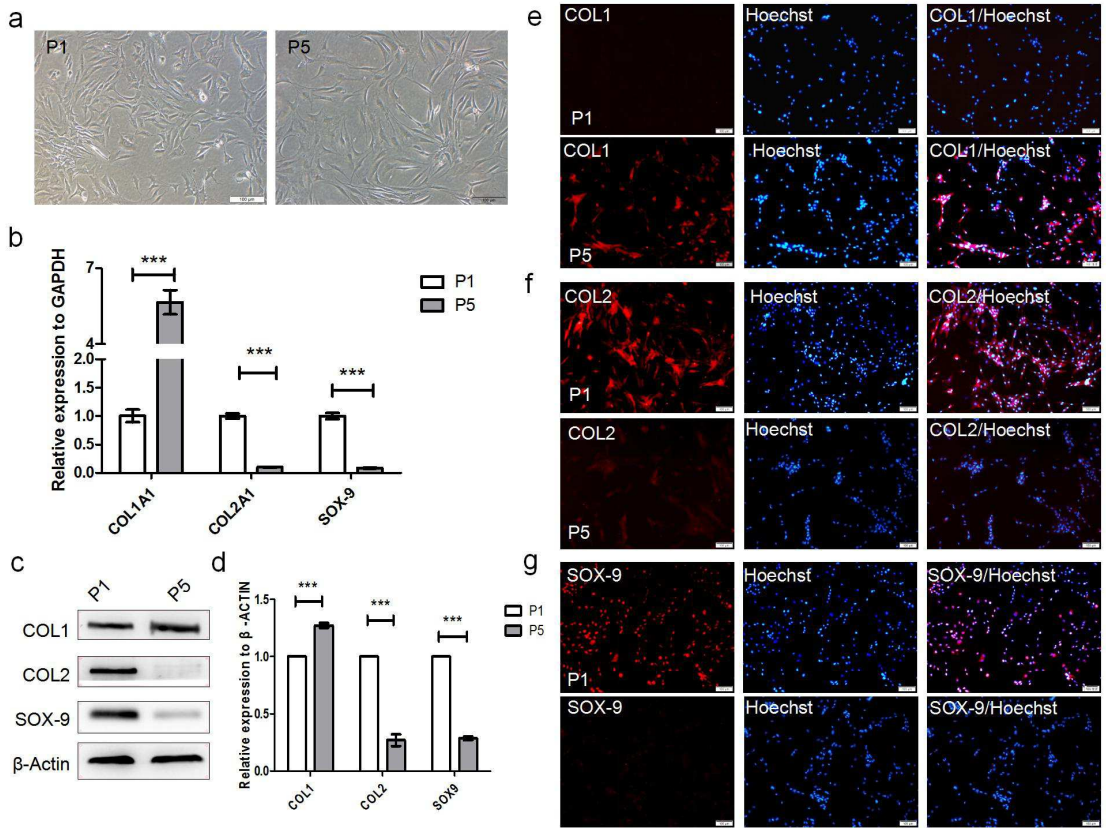

638

639 Figure 1. The dedifferentiation of human hyaline chondrocytes occurred during
640 passage culture in vitro. a: Morphological observation of chondrocytes of passage 1
641 (P1) and P5 chondrocytes. b: Real-time quantitative PCR (real-time qPCR) results of
642 *COL1A1* (alpha-1 type I collagen), *COL2A1*, and SOX-9 in P1 and P5 chondrocytes.
643 *GAPDH* (glyceraldehyde-3-phosphate dehydrogenase) was used as the internal
644 reference. Data are represented as the means ± standard deviation (n=3). c,d: Western

645 blot of COL1, COL2, and SOX-9 in P1 and P5 chondrocytes. β-actin was used as the
646 internal reference. e-g: Immunofluorescence of COL1, COL2, and SOX-9. *P<0.05,
647 **P<0.01, ***P<0.001. Scale bar, 100μm.

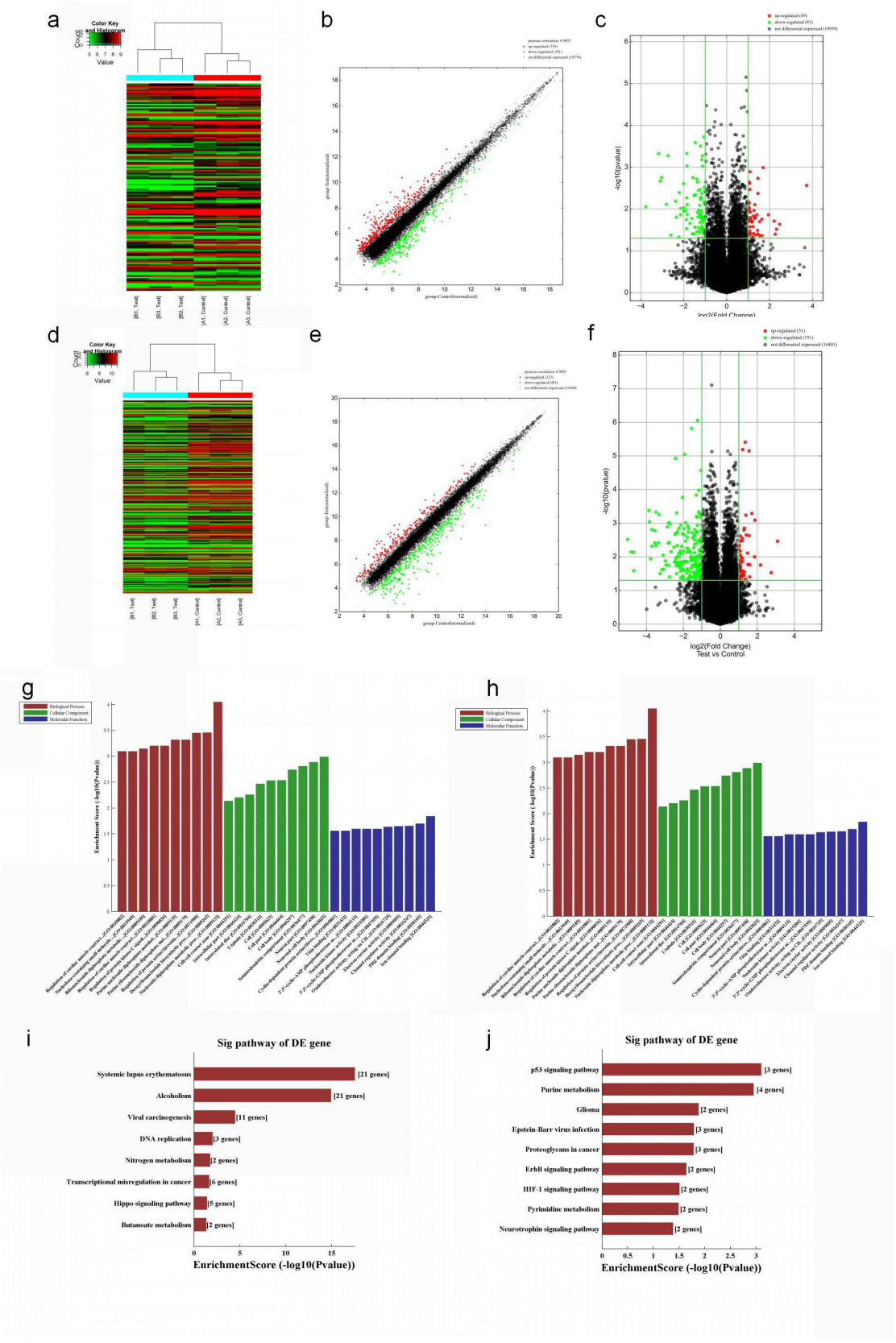

Figure 2. The results of high-throughput sequencing of lncRNAs (long non-coding RNA) and mRNAs in P1 and P5 chondrocytes (P1: A1, A2, A3; P5: B1, B2, B3). a:

Thermal map, b: scatter map, and c: volcanic map of lncRNAs. d: Thermal map, e: scatter plot, and f: volcano plot of mRNAs. Green dots represent downward adjustment, red dots represent upward adjustment, and black dots represent no significant change. g: Compared with P1 chondrocytes, the typical downregulated biological processes, cellular components, and molecular functions in P5 chondrocytes. h: The typical upregulated biological processes, cellular components, and molecular functions in P5 chondrocytes. i: The typical downregulated pathways in P5 chondrocytes. j: The typical upregulated pathways in P5 chondrocytes.

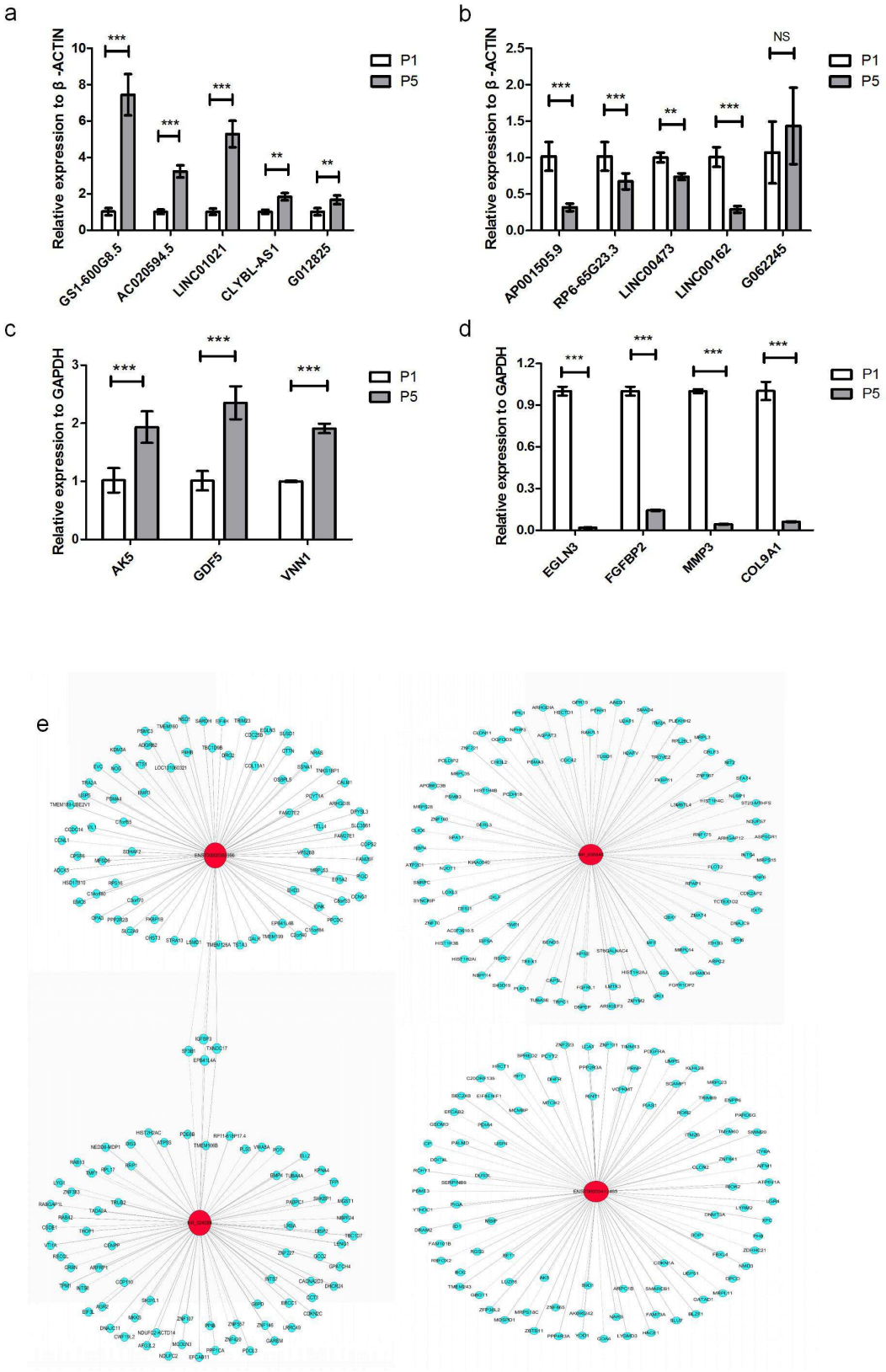

659

660 Figure 3. LncRNAs and mRNAs were selected for real-time qPCR verification. a:

661 Real-time qPCR results of five upregulated lncRNAs. b: Real-time qPCR results of

five downregulated lncRNAs. c: Real-time qPCR results of three upregulated mRNAs. d: Real-time qPCR results of four downregulated mRNAs. e: Co-expression network analysis of lncRNAs and mRNAs, red circle represents lncRNAs, blue circle represents mRNAs, solid line represents positive regulation, and dotted line represents negative regulation. *GAPDH* and *β-actin* were used as the internal references. Data are represented as means ± standard deviation (n=3). *P<0.05, **P<0.01, ***P<0.001. NS, not significant.

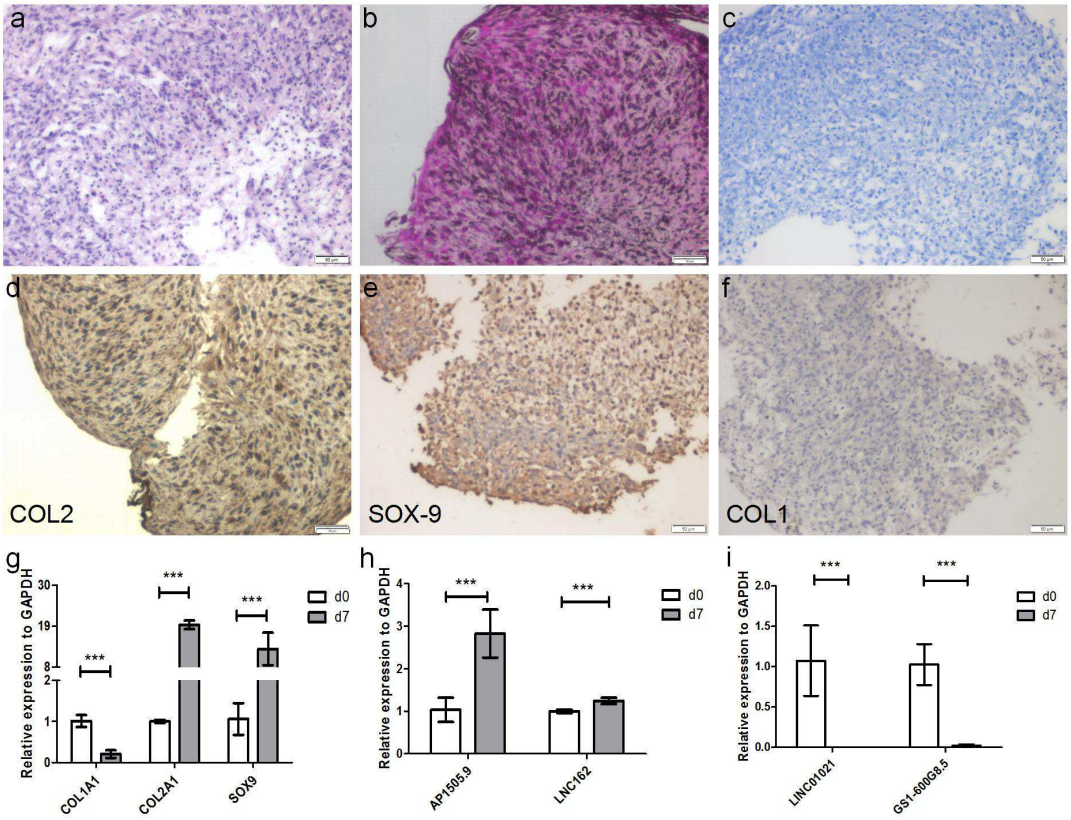

Figure 4. Pellet culture of P5 chondrocytes for seven days made chondrocytes undergo redifferentiation. a: Hematoxylin-eosin (HE) staining results. b: The results of safranin O staining. c: The results of Alcian staining. d: Immunohistochemistry of COL2. e: Immunohistochemistry of SOX-9. f: Immunohistochemistry of COL1. g: Real-time qPCR of cartilage-related marker genes (*COL1A1*, *COL2A1*, and *SOX-9*).

h,i: Real-time qPCR of lncRNAs (AP001505.9, LINC00162, LINC01021, and GS1-600G8.5). *GAPDH* was used as the internal reference. Data are represented as means ± standard deviation. *P<0.05, **P<0.01, ***P<0.001. Scale bar, 50μm.

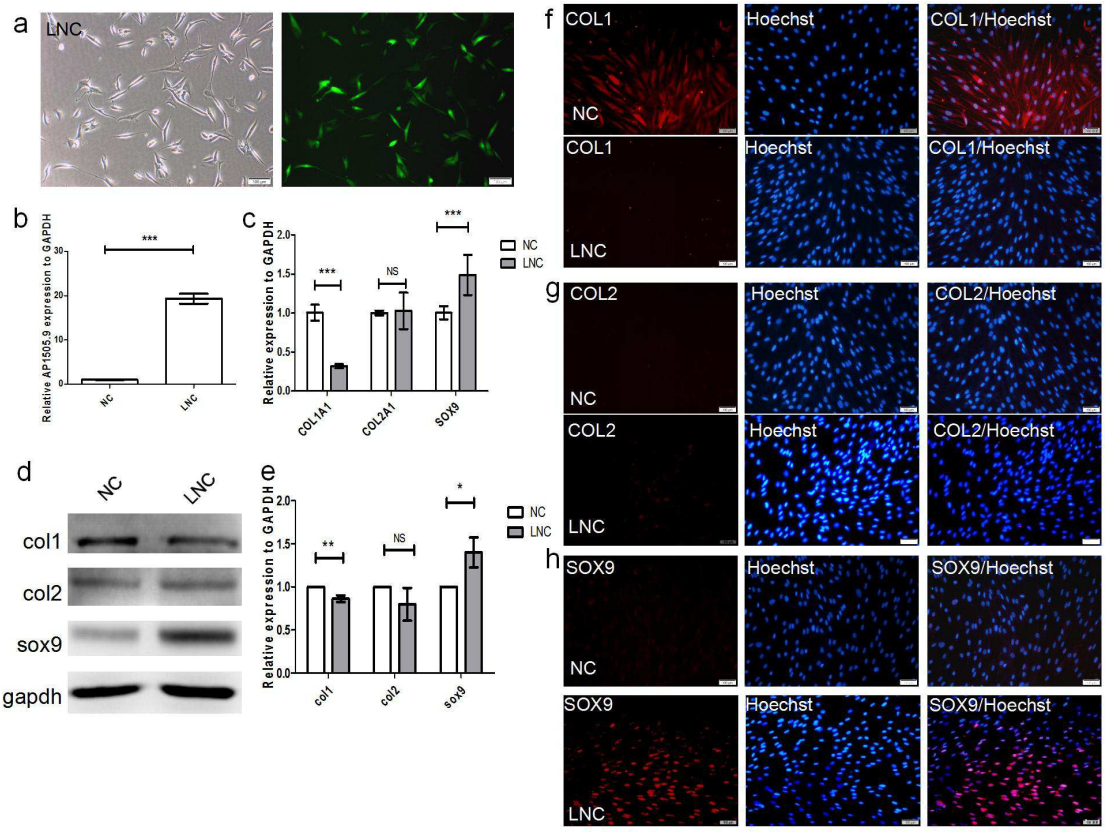

Figure 5. Lentiviral transfection experiments show the overexpression of AP001505.9. a: The results of phase contrast microscopy and fluorescence microscopy. Green fluorescence represents the successful chondrocyte transfected by lentivirus. LNC represented the chondrocyte transfected by AP001505.9 lentivirus. NC represented the chondrocyte transfected by negative control lentivirus b: Real-time qPCR of AP001505.9. c: Real-time qPCR of *COL1A1*, *COL2A1*, and *SOX*-9. d,e: Western blot of COL1, COL2, and SOX-9. f-h: Immunofluorescence of COL1, COL2, and SOX-9. *GAPDH* was used as the internal reference. Data are represented as means ± standard deviation. *P<0.05, **P<0.01, ***P<0.001. NS, not significant. Scale bar, 100μm.

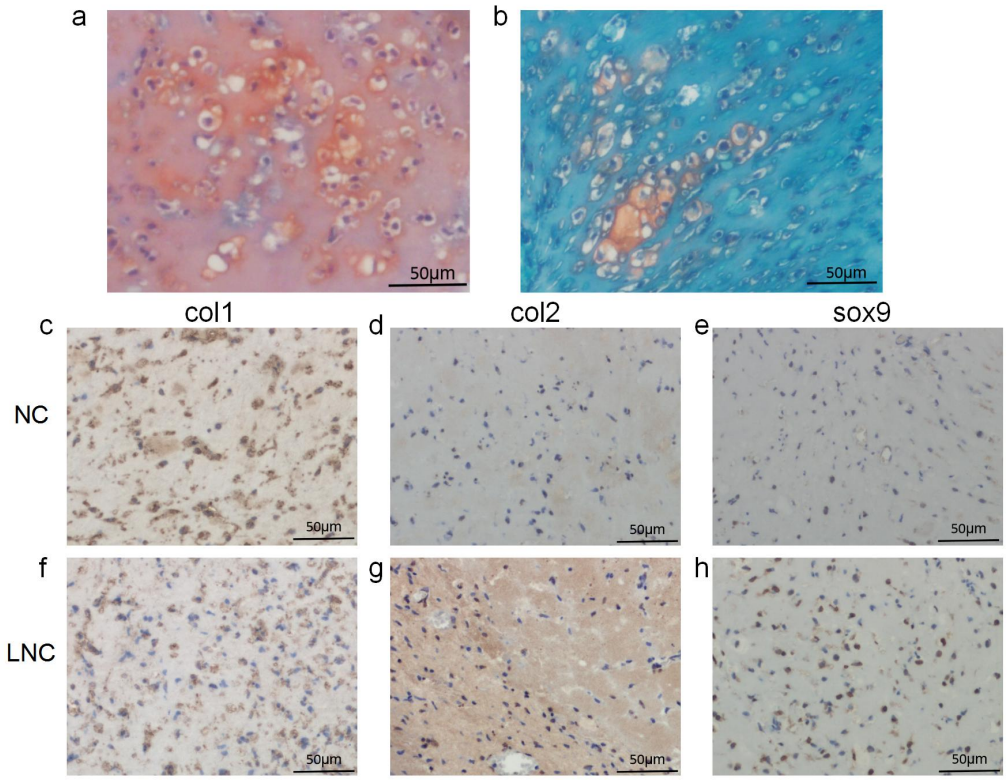

688

689 Figure 6. Results of histology and immunohistochemistry in vivo four weeks after
690 transplantation. a, b: The results of safranin O staining. Immunohistochemistry of (c, f)
691 COL1, (d, g) COL2, and (e, h) SOX-9. LNC represented the chondrocyte transfected
692 by AP001505.9 lentivirus. NC represented the chondrocyte transfected by negative
693 control lentivirus. Scale bar, 50μm.

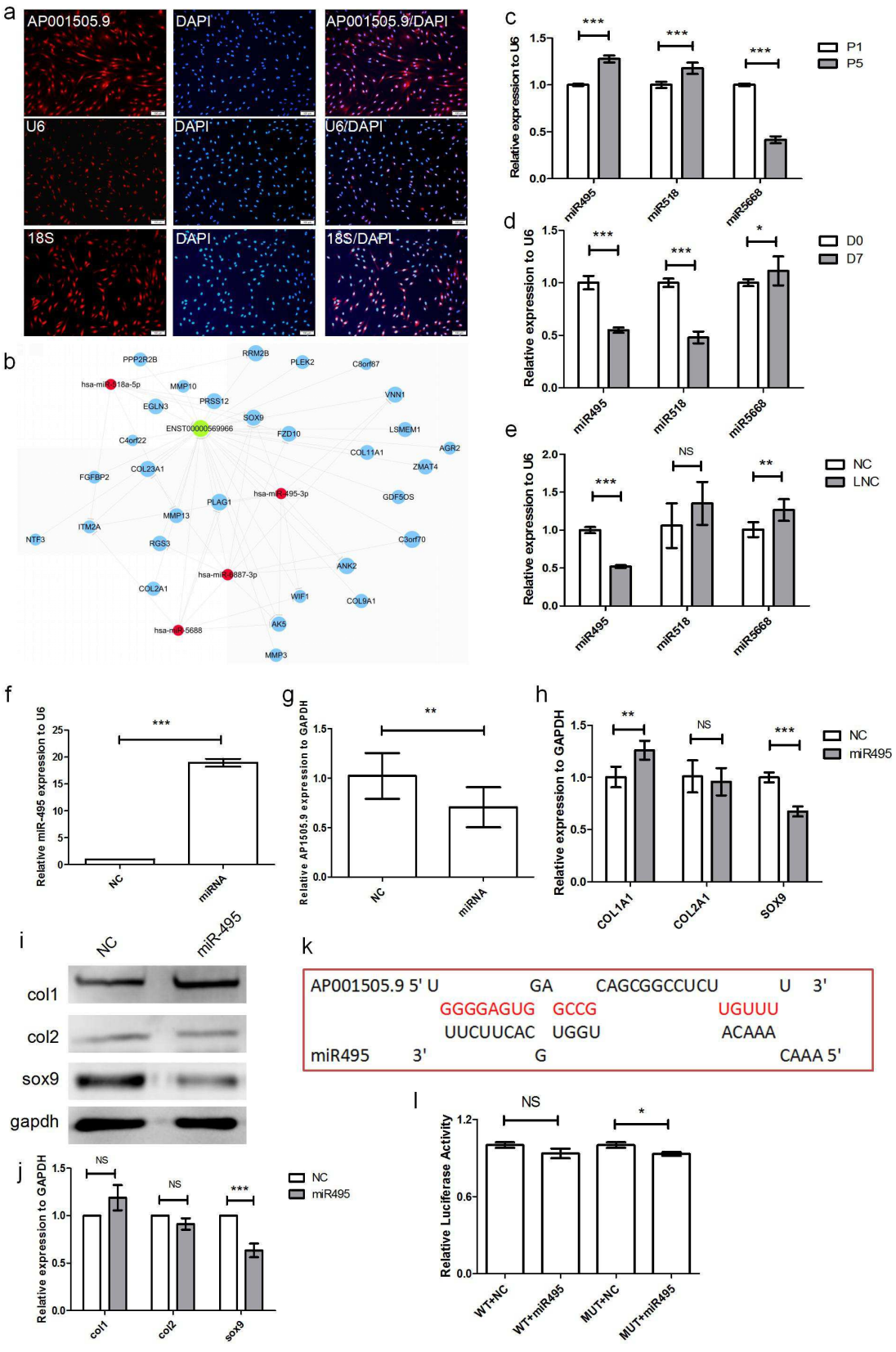

Figure 7. Mechanism of AP001505.9 inhibiting dedifferentiation. a: Fluorescence in situ hybridization of AP001505.9. U6 and 18S were used as internal reference probes

in nucleus and cytoplasm. b: Competing endogenous RNA (ceRNA) analysis of AP001505.9, the blue circles represent cartilage-related genes, the red circles represent miRNAs, and the green circles represent lncRNAs. c: Real-time qPCR of miRNAs in dedifferentiation. d: Real-time qPCR of miRNAs in redifferentiation. e: Real-time qPCR of miRNAs after AP001505.9 overexpression. f: Real-time qPCR of miR-495. G: qRT-PCR of AP001505.9 after miR-495 overexpression. h: Real-time qPCR of *COL1A1*, *COL2A1*, and *SOX-9* after miR-495 overexpression. i, j: Western blot of COL1, COL2, and SOX-9 after miR-495 overexpression. k: Potential binding sites of AP001505.9 and miR-495. l: Double luciferase experiment of AP001505.9 and miR-495. LNC represented the chondrocyte transfected by AP001505.9 lentivirus. miR495 represented the chondrocyte transfected by miR-495 mimic. NC represented the chondrocyte transfected by negative control lentivirus or mimic. *GAPDH* was used as the internal reference. Data are represented as means ± standard deviation. *P<0.05, **P<0.01, ***P<0.001. NS, not significant. Scale bar, 100μm.

Supplemental Information:

Table S1. Primers used in mRNA and lncRNA real-time qPCR.

Gene name	Sequences of primers
COL1A1	F:5'GTTGCTGCTTGCAGTAACCTT3'
	R:5'AGGGCCAAGTCCAACTCCTT3'
COL2A1	F:5'TGGACGATCACGAAACC3'
	R:5'GCTGCGGATGCTCTCAATCT3'

SOX-9	F:5’AGCGAACGCACATCAAGAC3’ R:5’CTGTAGGCGATCTGTTGGGG3’
AK5	F:5’GCAGAGCAAATTATGAGC3’ R:5’TAGCTGGGAAGCAAACAGT3’
VNN1	F:5’CCGCTAGCACCATGACTACTC3’ R:5’GCTCGAGCTACCAACTTAATGA3’
GDF5	F:5’CGATAAGACCGTGTATGAGT3’ R:5’CTCGCAGTGGAAAGCCTCGT3’
EGLN3	F:5’CATCAGCTTCCTCCTGTC3’ R:5’CCACCATTGCCTTAGACC3’
FGFBP2	F:5’TGGGAACATTGTTGGAAACC3’ R:5’GGTTGTCTGTCAGGGAGAGG3’
MMP3	F:5’AGTCTTCCAATCCTACTGTTGCT3’ R:5’TCCCCGTCACCTCCAATCC3’
COL9A1	F;5’TCGATGGCTTTGCTGTGCTGGG3’ R:5’TGGGTCGCAGGGGGTCACAAT3’
CLYBL-AS1	F:5'ACCAAGAAGCAGGATAGTTAGG3’ R:5’ TGCCAGGCTCATTGTCATA3’
LINC01021	F:5' ACTGACCCTTCAATGTGCCC3’ R:5’ CATTTCTCAAGCCCCGTGTT3’
AP001505.9	F:5'GCCTCTTGTTTTCCTTCCC3’ R:5’ TGCTTCGTGGTGAGACTCCT3’

RP6-65G23.3	F:5'CTCCCCTTTATGAGGACTGC3’ R:5’ CTCAGCATGGTTGTAAGCAGTA3’
G012825	F:5'CTTCCTACTCCAGGTAAACCC3’ R:5’ TCTCCATCAGCAGTCCAAAC3’
G062245	F:5'CCCAGTAGGAGGATAGTCAAGG3’ R:5’ TGTGGTGATGGGACTTCGTG3’
AC020594.5	F:5'CGCCCACTACAGGAAATGAAG3’ R:5’ CCACGGGACAAATACTACTCAGA 3’
LINC00473	F:5'AGCCAAAAGGGTTTAGAGTCAG3’ R:5’ GAGCAGGTAGGGAAATGATGTT3’
LINC00162	F:5'CGCTGAACTGCCTGGACTTT3’ R:5’ TGTGCGGTCTCCTCTTGGGT3’
GS1-600G8.5	F:5'CGGGGAGTCTTGAGAATGGG3’ R:5’ TAATCAGGCCGGAGTTGCA3’
GAPDH	F:5’CGCTCTCTGCTCCTCCTGTT3’ R:5’ CCATGGTGTCTGAGCGATGT3’
β-Actin	F:5’GTGGCCGAGGACTTTGATTG3’ R:5’CCTGTAACAACGCATCTCATATT3’

713

714 Table S2. Primers used in microRNA real-time qPCR.

microRNA	Source	Identifier

hsa-miR-518a-5p	GeneCopoeia	HmiRQP0579
hsa-miR-495-3p	GeneCopoeia	HmiRQP0537
hsa-miR-5668	GeneCopoeia	HmiRQP2716
snRNA U6	GeneCopoeia	HmiRQP9001

715

716 Table S3. Top 20 differentially expressed lncRNAs in human chondrocyte
717 dedifferentiation in vitro.

Seqname	**GeneSymbol**	**Fold Change**	**Regulation**
ENST00000610087	RP11-53B2.6	13.61615	down
NR_024089	LINC00162	9.0286718	down
T117110	G027615	8.539106	down
ENST00000605537	RP4-555D20.3	8.1710518	down
NR_026860	LINC00473	7.0314198	down
ENST00000525376	AF186192.1	6.6547277	down
T166066	G038554	6.0541931	down
NR_046283	NEBL-AS1	5.1958752	down
NR_027082	SFTA1P	5.0757797	down
ENST00000554032	RP6-65G23.3	4.6948336	down
T009872	G002089	4.6358255	down
NR_033997	RNF144A-AS1	4.4444077	down

ENST00000569966	AP001505.9	4.3928127	down
ENST00000608286	LL22NC03-N14H11.1	4.0253927	down
T117111	G027616	4.0109597	down
NR_036503	PRKCQ-AS1	3.969014	down
T268788	G062245	3.7967111	down
T327661	G076785	3.6682149	down
ENST00000603720	RP11-297J22.1	3.6442772	down
TCONS_00006002	XLOC_002629	3.6380732	down
NR_038848	LINC01021	13.268177	up
uc001szi.3	AK022997	5.5453205	up
NR_120384	CLYBL-AS1	5.0195295	up
T214806	G049673	4.8163804	up
T191664	G044136	4.6401846	up
ENST00000412485	GS1-600G8.5	3.8646113	up
NR_036540	LINC00622	3.2450684	up
ENST00000609674	RP11-563K23.1	3.1289083	up
uc.185-	uc.185	3.1146988	up
ENST00000451982	LINC00969	2.9062816	up
T328268	G076957	2.8993137	up
ENST00000573950	TAPT1-AS1	2.7537015	up
ENST00000608605	RP11-804H8.6	2.7520865	up
uc003ifn.3	AK090904	2.7447524	up

T132722	G031137	2.7103456	up
ENST00000423781	AC004870.4	2.6490488	up
uc.185+	uc.185	2.5668814	up
NR_024006	LINC00950	2.5124995	up
NR_120623	TCERG1L-AS1	2.4902614	up
NR_131012	NEAT1	2.4842201	up

718

719 Table S4. Significant differentially expressed mRNAs in human chondrocyte
720 dedifferentiation in vitro.

Seqname	**GeneSymbol**	**Fold Change**	**Regulation**
NM_022073	EGLN3	32.531482	down
NM_031950	FGFBP2	28.505518	down
NM_002422	MMP3	25.838385	down
NM_001851	COL9A1	25.715546	down
NM_006408	AGR2	14.594614	down
NM_004867	ITM2A	14.22944	down
NM_002425	MMP10	13.706152	down
NM_016445	PLEK2	13.044514	down
NM_173662	RNF175	12.99444	down
NM_001242668	C8orf87	11.733266	down
NM_152770	C4orf22	8.5786754	up

NM_003619	PRSS12	6.766859	up
NM_174858	AK5	4.5321298	up
NM_004666	VNN1	3.6649314	up
ENST00000374375	GDF5OS	3.6237528	up
NM_001148	ANK2	3.2715659	up
NM_144488	RGS3	3.0256487	up
NM_002655	PLAG1	3.0189914	up
NM_015713	RRM2B	2.9571532	up
NM_182597	LSMEM1	2.9430627	up

721

Figures

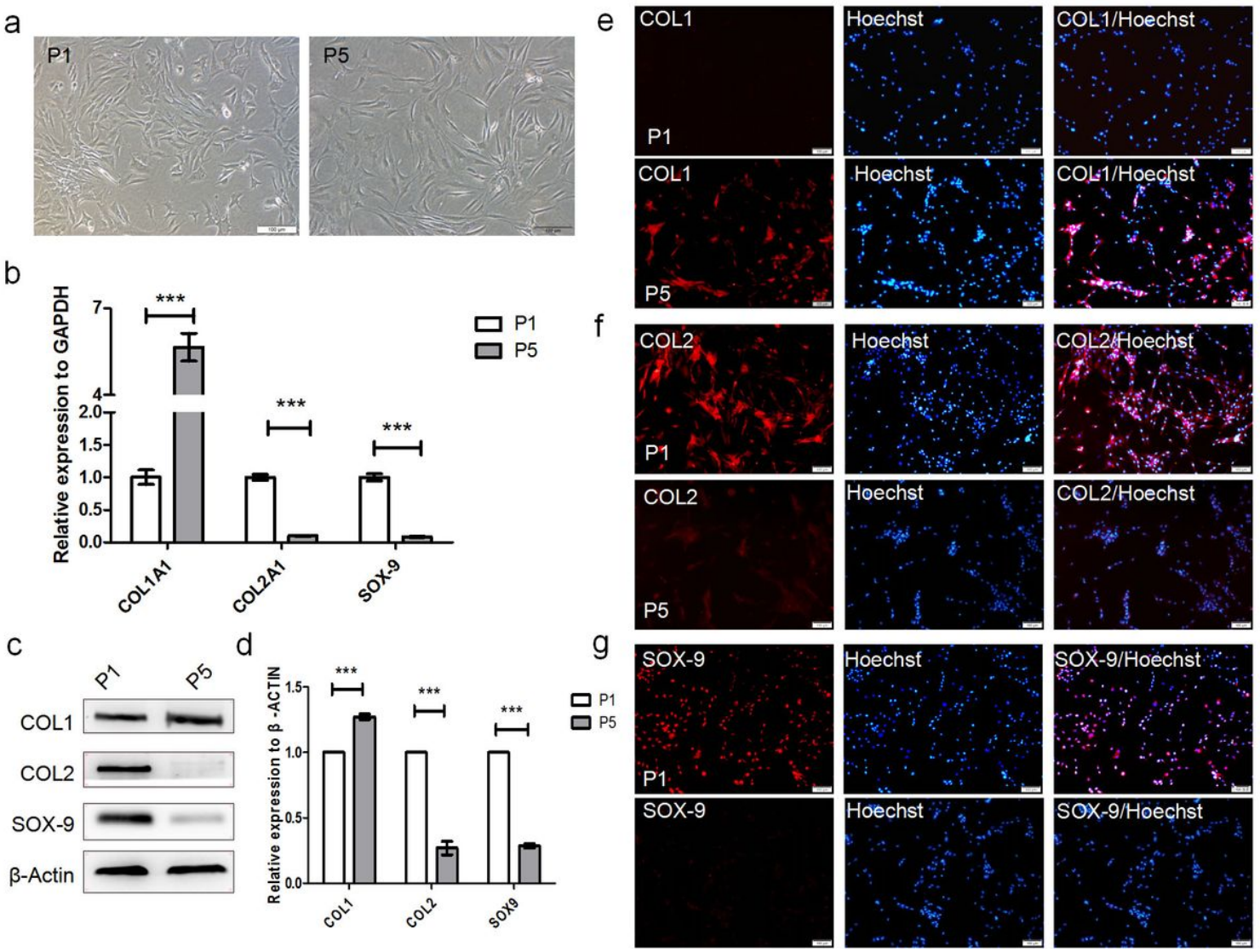

Figure 1

The dedifferentiation of human hyaline chondrocytes occurred during passage culture in vitro. a: Morphological observation of chondrocytes of passage 1 (P1) and P5 chondrocytes. b: Real-time quantitative PCR (real-time qPCR) results of COL1A1 (alpha-1 type I collagen), COL2A1, and SOX-9 in P1 and P5 chondrocytes. GAPDH (glyceraldehyde-3-phosphate dehydrogenase) was used as the internal reference. Data are represented as the means ± standard deviation (n=3). c,d: Western blot of COL1, COL2, and SOX-9 in P1 and P5 chondrocytes. β-actin was used as the internal reference. e-g: Immunofluorescence of COL1, COL2, and SOX-9. *P<0.05, **P<0.01, ***P<0.001. Scale bar, 100μm.

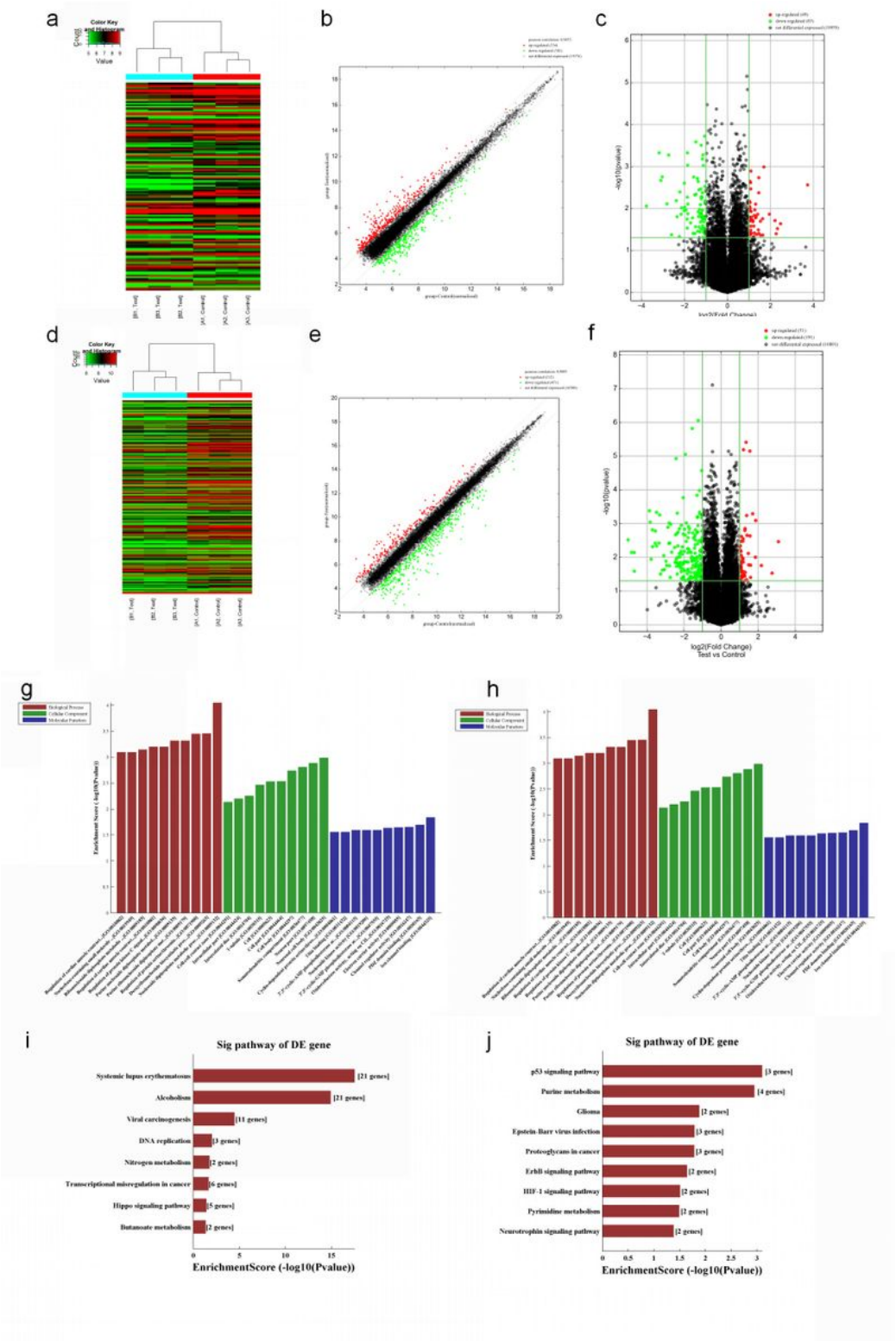

Figure 2

The results of high-throughput sequencing of lncRNAs (long non-coding RNA) and mRNAs in P1 and P5 chondrocytes (P1: A1, A2, A3; P5: B1, B2, B3). a: Thermal map, b: scatter map, and c: volcanic map of lncRNAs. 651 d: Thermal map, e: scatter plot, and f: volcano plot of mRNAs. Green dots represent downward adjustment, red dots represent upward adjustment, and black dots represent no significant change. g: Compared with P1 chondrocytes, the typical downregulated biological processes, cellular

components, and molecular functions in P5 chondrocytes. h: The typical upregulated biological processes, cellular components, and molecular functions in P5 chondrocytes. i: The typical downregulated pathways in P5 chondrocytes. j: The typical upregulated pathways in P5 chondrocytes.

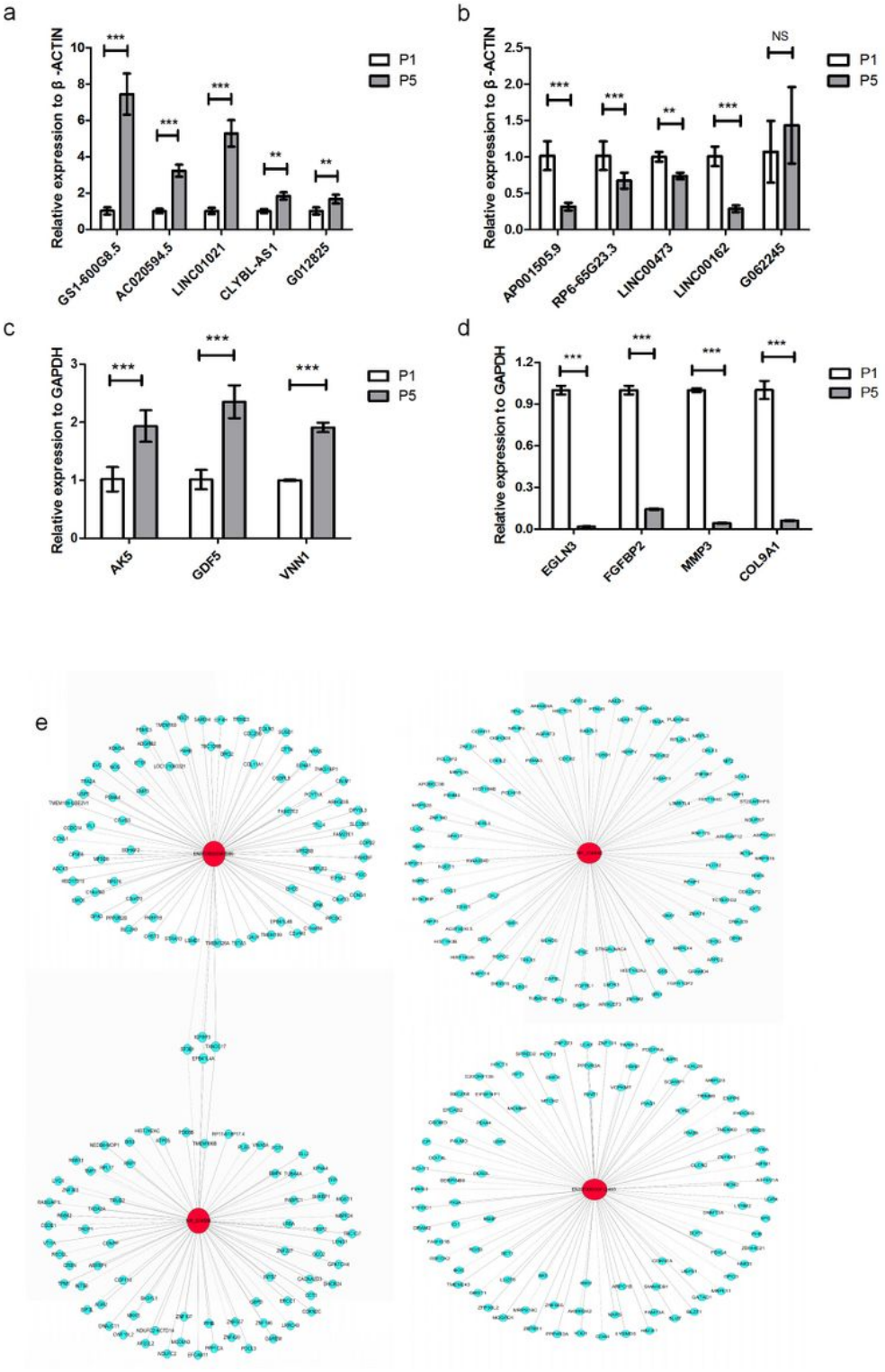

Figure 3

LncRNAs and mRNAs were selected for real-time qPCR verification. a: Real-time qPCR results of five upregulated lncRNAs. b: Real-time qPCR results of five downregulated lncRNAs. c: Real-time qPCR results

of three upregulated mRNAs. d: Real-time qPCR results of four downregulated mRNAs. e: Co-expression network analysis of lncRNAs and mRNAs, red circle represents lncRNAs, blue circle represents mRNAs, solid line represents positive regulation, and dotted line represents negative regulation. GAPDH and β-actin were used as the internal references. Data are represented as means ± standard deviation (n=3). *P<0.05, **P<0.01, ***P<0.001. NS, not significant.

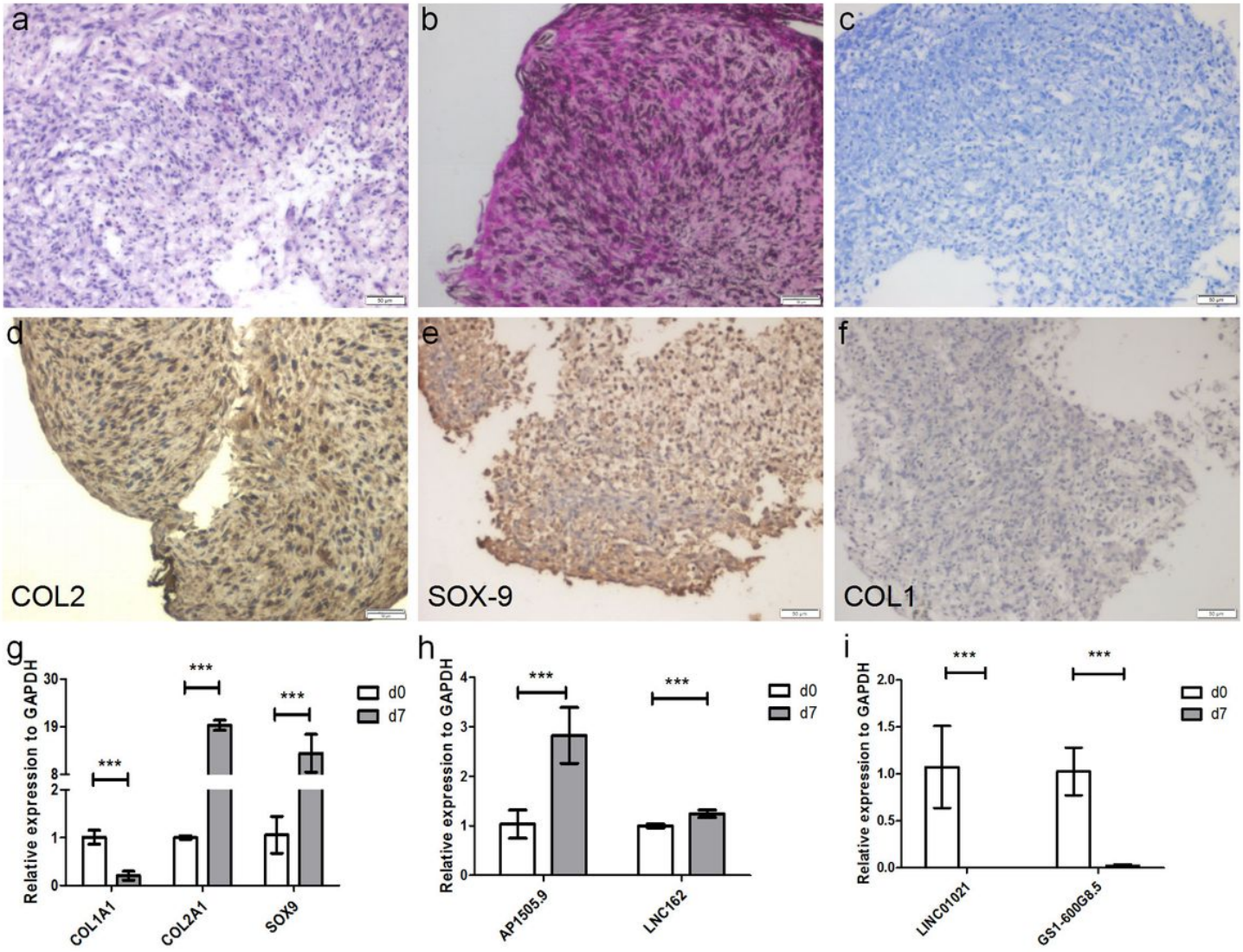

Figure 4

Pellet culture of P5 chondrocytes for seven days made chondrocytes undergo redifferentiation. a: Hematoxylin-eosin (HE) staining results. b: The results of safranin O staining. c: The results of Alcian staining. d: Immunohistochemistry of COL2. e: Immunohistochemistry of SOX-9. f: Immunohistochemistry of COL1. g: Real-time qPCR of cartilage-related marker genes (COL1A1, COL2A1, and SOX-9). h,i: Real-time qPCR of lncRNAs (AP001505.9, LINC00162, LINC01021, and GS1-600G8.5). GAPDH was used as the internal reference. Data are represented as means ± standard deviation. *P<0.05, **P<0.01, ***P<0.001. Scale bar, 50μm.

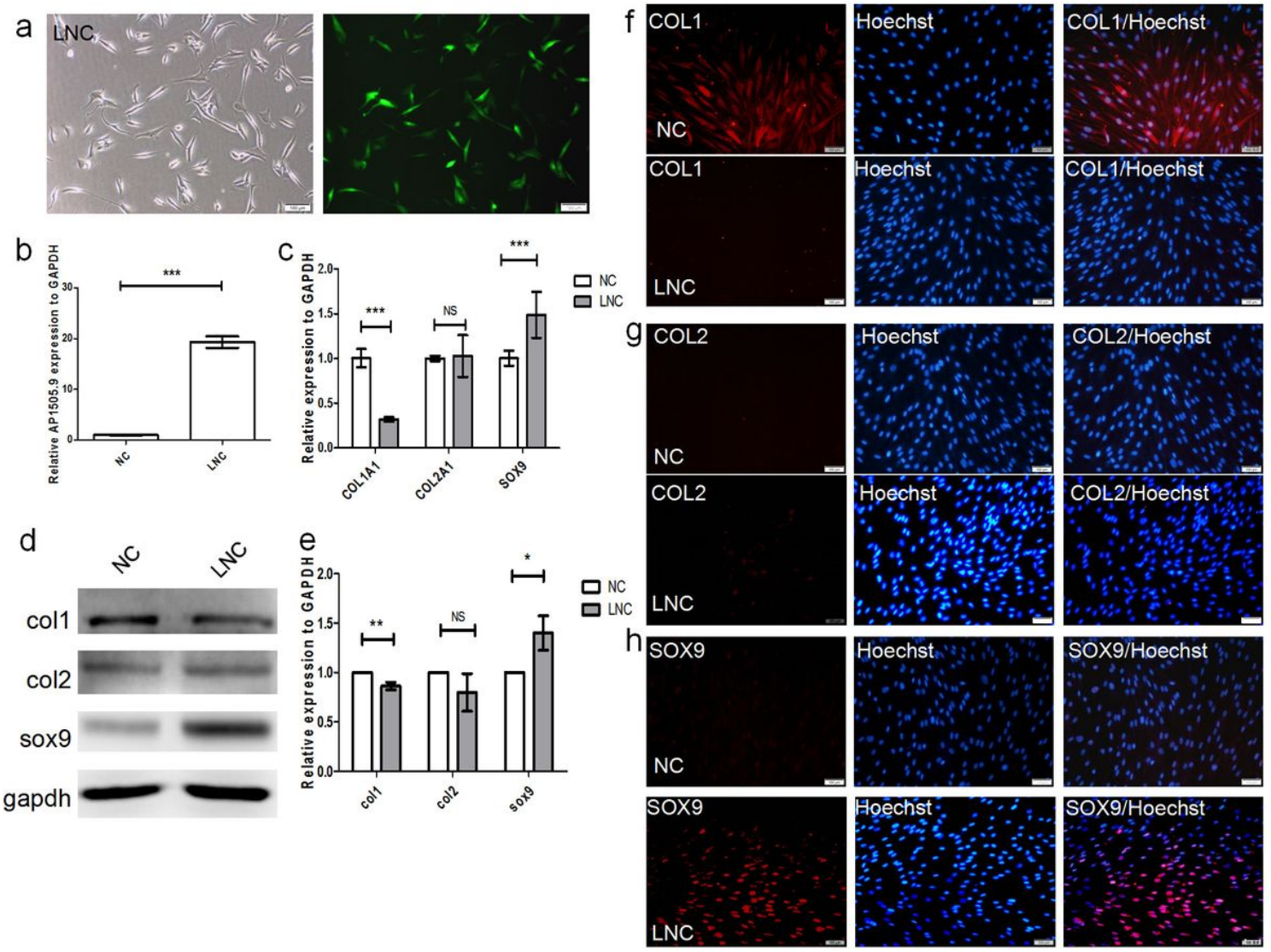

Figure 5

Lentiviral transfection experiments show the overexpression of AP001505.9. a: The results of phase contrast microscopy and fluorescence microscopy. Green fluorescence represents the successful chondrocyte transfected by lentivirus. LNC represented the chondrocyte transfected by AP001505.9 lentivirus. NC represented the chondrocyte transfected by negative control lentivirus b: Real-time qPCR of AP001505.9. c: Real-time qPCR of COL1A1, COL2A1, and SOX-9. d,e: Western blot of COL1, COL2, and SOX-9. f-h: Immunofluorescence of COL1, COL2, and SOX-9. GAPDH was used as the internal reference. Data are represented as means ± standard deviation. *P<0.05, **P<0.01, ***P<0.001. NS, not significant. Scale bar, 100μm.

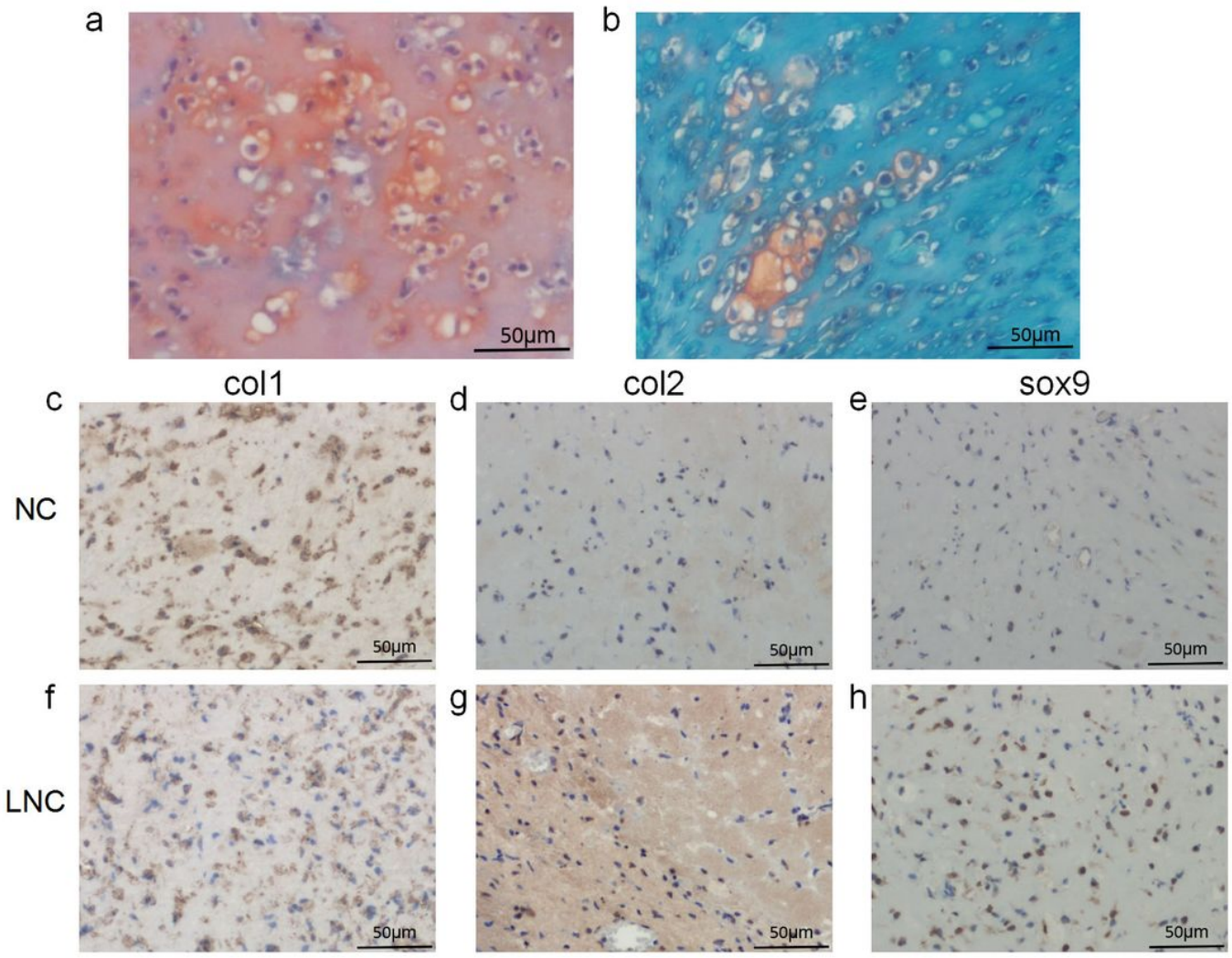

Figure 6

Results of histology and immunohistochemistry in vivo four weeks after transplantation. a, b: The results of safranin O staining. Immunohistochemistry of (c, f) COL1, (d, g) COL2, and (e, h) SOX-9. LNC represented the chondrocyte transfected by AP001505.9 lentivirus. NC represented the chondrocyte transfected by negative control lentivirus. Scale bar, 50μm.

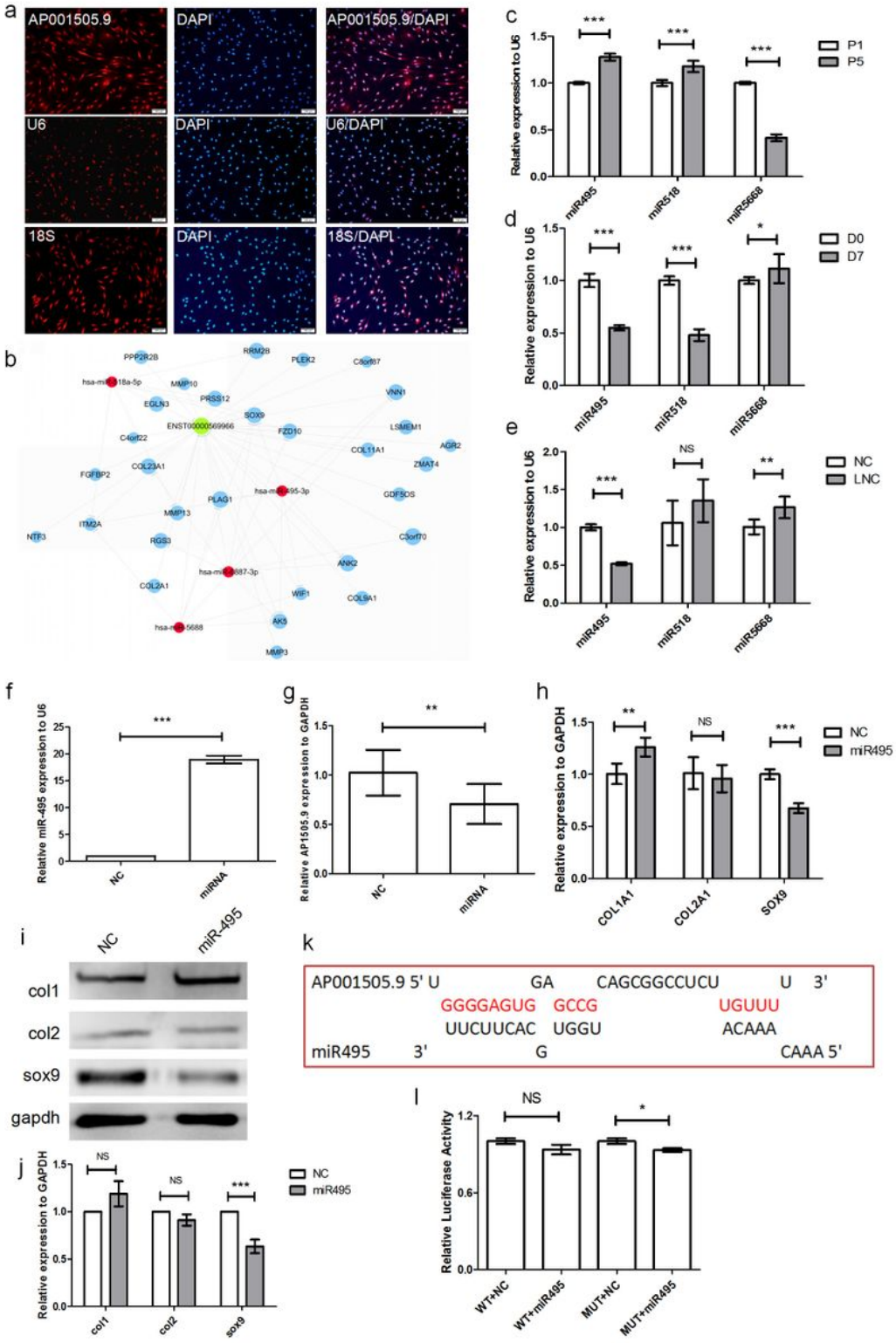

Figure 7

Mechanism of AP001505.9 inhibiting dedifferentiation. a: Fluorescence in situ hybridization of AP001505.9. U6 and 18S were used as internal reference probes in nucleus and cytoplasm. b: Competing endogenous 697 RNA (ceRNA) analysis of AP001505.9, the blue circles represent cartilage-related genes, the red circles represent miRNAs, and the green circles represent lncRNAs. c: Real-time qPCR of miRNAs in dedifferentiation. d: Real-time qPCR of miRNAs in redifferentiation. e: Real-time qPCR of miRNAs after

AP001505.9 overexpression. f: Real-time qPCR of miR-495. G: qRT-PCR of AP001505.9 after miR-495 overexpression. h: Real-time qPCR of COL1A1, COL2A1, and SOX-9 after miR-495 overexpression. i, j: Western blot of COL1, COL2, and SOX-9 after miR-495 overexpression. k: Potential binding sites of AP001505.9 and miR-495. l: Double luciferase experiment of AP001505.9 and miR-495. LNC represented the chondrocyte transfected by AP001505.9 lentivirus. miR495 represented the chondrocyte transfected by miR-495 mimic. NC represented the chondrocyte transfected by negative control lentivirus or mimic. GAPDH was used as the internal reference. Data are represented as means ± standard deviation. *P<0.05, **P<0.01, ***P<0.001. NS, not significant. Scale bar, 100μm.

Supplementary Files

This is a list of supplementary files associated with this preprint. Click to download.

- arrive.pdf